Earth Syst. Sci. Data, 9, 927–953, 2017
https://doi.org/10.5194/essd-9-927-2017

Open Access Earth System Science Data

Anthropogenic land use estimates for the Holocene – HYDE 3.2

Kees Klein Goldewijk[1,3], Arthur Beusen[2,3], Jonathan Doelman[3], and Elke Stehfest[3]

[1]Copernicus Institute of Sustainable Development, Utrecht University, Utrecht, P.O. Box 80115, the Netherlands
[2]Department of Earth Sciences, Utrecht University, Utrecht, P.O. Box 80115, the Netherlands
[3]PBL Netherlands Environmental Assessment Agency, The Hague, the Netherlands

Correspondence to: Kees Klein Goldewijk (c.g.m.kleingoldewijk@uu.nl)

Received: 21 November 2016 – Discussion started: 7 December 2016
Revised: 28 September 2017 – Accepted: 10 October 2017 – Published: 1 December 2017

Abstract. This paper presents an update and extension of HYDE, the History Database of the Global Environment (HYDE version 3.2). HYDE is an internally consistent combination of historical population estimates and allocation algorithms with time-dependent weighting maps for land use. Categories include cropland, with new distinctions for irrigated and rain-fed crops (other than rice) and irrigated and rain-fed rice. Grazing lands are also provided, divided into more intensively used pasture and less intensively used rangeland, and further specified with respect to conversion of natural vegetation to facilitate global change modellers. Population is represented by maps of total, urban, rural population, population density and built-up area. The period covered is 10 000 before Common Era (BCE) to 2015 Common Era (CE). All data can be downloaded from https://doi.org/10.17026/dans-25g-gez3.

We estimate that global population increased from 4.4 million people (we also estimate a lower range < 0.01 and an upper range of 8.9 million) in 10 000 BCE to 7.257 billion in 2015 CE, resulting in a global population density increase from 0.03 persons (or capita, in short cap) km^{-2} (range 0–0.07) to almost 56 cap km^{-2} respectively. The urban built-up area evolved from almost zero to roughly 58 Mha in 2015 CE, still only less than 0.5 % of the total land surface of the globe.

Cropland occupied approximately less than 1 % of the global land area (13 037 Mha, excluding Antarctica) for a long time period until 1 CE, quite similar to the grazing land area. In the following centuries the share of global cropland slowly grew to 2.2 % in 1700 CE (ca. 293 Mha, uncertainty range 220–367 Mha), 4.4 % in 1850 CE (578 Mha, range 522–637 Mha) and 12.2 % in 2015 CE (ca. 1591 Mha, range 1572–1604 Mha). Cropland can be further divided into rain-fed and irrigated land, and these categories can be further separated into rice and non-rice. Rain-fed croplands were much more common, with 2.2 % in 1700 CE (289 Mha, range 217–361 Mha), 4.2 % (549 Mha, range 496–606 Mha) in 1850 CE and 10.1 % (1316 Mha, range 1298–1325 Mha) in 2015 CE, while irrigated croplands used less than 0.05 % (4.3 Mha, range 3.1–5.5 Mha), 0.2 % (28 Mha, range 25–31 Mha) and 2.1 % (277 Mha, range 273–278 Mha) in 1700, 1850 and 2015 CE, respectively. We estimate the irrigated rice area (paddy) to be 0.1 % (13 Mha, range 9–16 Mha) in 1700 CE, 0.2 % (28 Mha, range 26–31 Mha) in 1850 CE and 0.9 % (118 Mha, range 117–120 Mha) in 2015 CE.

The estimates for land used for grazing are much more uncertain. We estimate that the share of grazing land grew from 5.1 % in 1700 CE (667 Mha, range 507–820 Mha) to 9.6 % in 1850 CE (1192 Mha, range 1068–1304 Mha) and 24.9 % in 2015 CE (3241 Mha, range 3211–3270 Mha). To aid the modelling community we have divided land used for grazing into more intensively used pasture, less intensively used converted rangeland and less or unmanaged natural unconverted rangeland. Pasture occupied 1.1 % in 1700 CE (145 Mha, range 79–175 Mha), 1.9 % in 1850 CE (253 Mha, range 218–287 Mha) and 6.0 % (787 Mha, range 779–795 Mha) in 2015 CE, while rangelands usually occupied more space due to their occurrence in more arid regions and thus

lower yields to sustain livestock. We estimate converted rangeland at 0.6 % in 1700 CE (82 Mha range 66–93 Mha), 1 % in 1850 CE (129 Mha range 118–136 Mha) and 2.4 % in 2015 CE (310 Mha range 306–312 Mha), while the unconverted natural rangelands occupied approximately 3.4 % in 1700 CE (437 Mha, range 334–533 Mha), 6.2 % in 1850 CE (810 Mha, range 733–881 Mha) and 16.5 % in 2015 CE (2145 Mha, range 2126–2164 Mha).

1 Introduction

Humans have emerged as the most important driving force of landscape transformation (Butzer, 1964; Ellis, 2015; Ellis et al., 2013; Kaplan et al., 2011). Long before the start of the Holocene, humans used fire as a tool to open up the landscape for grazing of wildlife to facilitate easier hunting. Then, roughly 12 000 years ago, the domestication of plants and animals slowly started and sedentary agriculture became more and more widespread. This led to conversion of natural ecosystems to other types of land use such as cropland, grazing land for livestock and built-up areas, a process that has accelerated greatly during the past few hundred years. This has led to the current situation in which more than 37 % of the ice-free land in the world is used for agriculture or settlements and another 30 % is more or less under the influence of humans, causing many natural resources to be heavily used or even near depletion (Ellis et al., 2013; Foley et al., 2005).

Land use plays an important role in the climate system (Feddema et al., 2005; Le Quéré et al., 2015). Many ecosystem processes are directly or indirectly climate driven, and together with anthropogenic land cover changes (ALCCs), they determine how the land surface will evolve over time (Betts, 2006; Brovkin et al., 2006; Claussen et al., 2001). The climate system is influenced in a biophysical manner by affecting radiative forcing through a changing albedo or heat fluxes (Matthews et al., 2003; Myhre and Myhre, 2003; Davin et al., 2007) but also through biogeochemical processes by exchanging greenhouse gases (GHGs) and other gases with the atmosphere (Betts, 2006; Brovkin et al., 2006; Betts et al., 2007). All these feedbacks on land use can be either positive or negative (Claussen et al., 2001).

ALCCs, mainly through conversion of undisturbed ecosystems to other land uses (e.g. deforestation for agriculture or grazing, forestry, or infrastructure), result in GHG emissions and have contributed considerably in the past to the cumulative carbon dioxide (CO_2) increase in the atmosphere. This part of the global carbon cycle is an important factor in the climate system and has been the focus of many studies (Feddema et al., 2005; Friedlingstein et al., 2006; Findell et al., 2007; Plattner et al., 2008; Strassmann et al., 2008). However, these carbon fluxes are still not well quantified in the global carbon budget (Le Quéré et al., 2015; Pacala et al., 2001). Uncertainties in quantifying the impact of land use changes on the global carbon cycle lead to uncertainties in projections of atmospheric CO_2 and climate and consequently affect policy makers in establishing reasonable emission mitigation strategies.

The existing global estimates of historical land use are rare and rather uncertain (Klein Goldewijk and Verburg, 2013). This can partly be explained by the sheer lack of reliable data, and hence by the different approaches used to reconstruct the trends, which vary from simple bookkeeping methods, to "hindcast" modelling techniques, to simulations of anthropogenic deforestation based on population densities (Houghton et al., 1983; Kaplan et al., 2011; Klein Goldewijk et al., 2011; Pongratz et al., 2008). The first analyses of carbon emissions from land use change were based on an approach that has come to be known as the bookkeeping approach (Houghton and Hackler, 2002; Houghton et al., 1983). This approach refers to the model used to calculate the changes in carbon following a change in land use. The model uses defined response curves (for four carbon pools: living biomass, woody debris, harvested wood products and soils) to determine the annual sources and sinks of carbon from each hectare undergoing a change related to management. The various uses of land in the first studies included croplands, pastures and the harvest of wood. Ramankutty and Foley (1999) present a study on global croplands only for the 1700–1992 CE period. They created a global representation of permanent croplands in 1992 CE, at 5 min spatial resolution, by calibrating a remotely sensed land cover classification data set against cropland inventory data. Next, they hindcasted the 1992 CE data with a simple land use change model back to 1700 CE. This was updated and expanded with pasture estimates for the 1700–2007 CE period (Ramankutty, 2012). Klein Goldewijk (2001) presented a reconstruction of croplands and pasture for the 1700–2000 CE period at a 30 arcmin resolution, which was updated to a 5 arcmin resolution and expanded to the 10 000 BCE to 2010 CE period (Klein Goldewijk et al., 2010, 2011). It primarily assumed a nearly constant per capita land use hindcasting approach, with changing allocation algorithms over time. Pongratz et al. (2008) presented a reconstruction of global agricultural areas for the 800–1992 CE period, the Millennium Land Cover Reconstruction (ML08). They aimed to provide spatially explicit maps at 0.5° resolution that reach further back in history than the data sets available at that time. The authors relied on existing land cover data where possible and used a wealth of literature on agricultural practices and agrotechnological innovations for all regions in the world; with this, per capita land use estimates could be accounted for

as evolving over time and at the same time changing differently in the different regions of the globe. They also used seven different population databases, and the upper and lower ends of uncertainties of per capita land use based on literature were applied. This led to two different trajectories of land cover change that reflect the upper and lower bounds within the uncertainty range of historical land cover changes, around a third, medium estimate that used a specific population data set and assumed constant per capita land use changes over time, which was a key shortcoming. The Kaplan and Krumhardt (KK10) scenario was developed to provide a basis for calculating the effects of anthropogenic land cover change on the global carbon cycle over the Holocene (Kaplan et al., 2011). The scenario is based on a non-linear empirical relationship between forest cover on land suitable for crop or pasture and country-level population density observed in Europe over the past 2 millennia on the basis of demographer estimates of population density and reconstructions of forest cover (Kaplan et al., 2011, 2009). The population density–forest cover relationship is approximated as a logistic function, with the most rapid rates of deforestation at intermediate aggregate population densities of ca. 50–100 persons per km^{-2}. This function results in an implied per capita land use that is a function of population density, which is further modulated by the potential suitability of the landscape for rain-fed agriculture, and pasture ALCC is still not successfully implemented in many models and studies of global change. As a result, climate modelling in paleo-mode or projection mode that tries to take ALCC into account is seriously hindered (Gaillard et al., 2010). The few scenarios of past ALCC that exist, e.g. ML08 (Pongratz et al., 2009), HYDE (Klein Goldewijk et al., 2011) and KK10 (Kaplan et al., 2011, 2009), show very large differences indeed (Gaillard et al., 2010). Therefore, improved descriptions of past anthropogenic land cover change on the global spatial scale are urgently needed.

This study presents a key update and extension of the former HYDE 3.1 historical land use database (Klein Goldewijk et al., 2010, 2011). This recent version, HYDE 3.2, is an improved and internally consistent combination of new historical population data and land use allocation algorithms, which vary over time. Categories include cropland, with a new distinction between irrigated and rain-fed crops (other than rice) and irrigated and rain-fed rice. In addition, grazing lands are provided and categorized into more intensively used pasture and less intensively used rangeland. Population is also represented by maps of total, urban, rural population and population density as well as built-up area. The period covered now is 10 000 BCE to 2015 CE.

An overview of the new features of HYDE 3.2 include

- improved allocation algorithms (a smoother transition from current "satellite-based" allocation towards "rule-based" allocation in the past);
- updated historical estimates of many land use categories (e.g. improved census data of 55 countries);
- a distinction between rain-fed and irrigated cropland;
- an introduction of the land use category rice (rain-fed and irrigated);
- the use of additional data (cropland layer map of Waldner et al., 2016; irrigation data of Siebert, 2008, and Siebert et al., 2015, MIRCA data set) and rice data from You et al., 2014);
- the use of the most recent and higher-resolution satellite information on land cover from the ESA consortium for 2010 reference maps;
- a new distinction between pasture and rangeland according to the intensity of use, and a further classification of rangeland into rangeland under natural vegetation and rangeland involving conversion of natural vegetation;
- an extension of the database to the year 2015.

2 Methodology and data

2.1 Input data for population

The basis for our population data is the United Nations World Populations Prospects (2008 Revision) for the 1950–2015 period. The pre-1950 historical estimates were largely taken from McEvedy and Jones (1978), Livi-Bacci (2007), and Maddison (2001). We supplemented them with the sub-national population numbers of Populstat (Lahmeyer, personal communication, 2004) and many other country-specific sources (see the Supplement A). Time series were constructed for each province or state of every country of the world. We used the current administrative units and kept them constant over time for simplicity reasons. Other historical sources were adjusted to match the current boundaries of HYDE 3.2 if needed by taking fractions of those former, often larger, administrative units (e.g. Roman Empire). The methodology is similar to that described in detail in Klein Goldewijk et al. (2010).

2.2 Spatial coverage for population

For the present, we used the spatial patterns from LandScan (2014) for the year 2012 in our weighting maps to allocate our total population for each administrative unit. LandScan, developed at the Department of Energy's Oak Ridge National Laboratory, USA, is a global population database showing population totals at 1 km resolution. The modelling process uses subnational-level census counts for each country and primary geospatial input or ancillary data sets, including land cover, roads, slope, urban areas, village locations and high-resolution imagery analysis.

2.3 Input data for land use

In this section, we describe the national and subnational data for all land use categories, from 10 000 BCE until present day, and the construction of land use maps for the present day. The allocation method to derive land use maps for the historic period back to 10 000 BCE is described in Sect. 3.2.

2.3.1 Cropland and grazing land statistics

We started with country totals for the FAO categories of "arable land and permanent crops" and "permanent meadows and pastures", further referred to here as "cropland" and "grazing land" respectively (FAO, 2015). The FAO data reach back to 1960, and thus for the period 1960–2015 CE, the FAO data were followed exactly, though complemented in some countries by subnational statistics. For the pre-1960 CE period another method had to be used, and we combined population estimates with per capita land use estimates. For 1960, per capita cropland and grazing land was derived from FAO data and then modelled back in time, assuming that they were not constant but followed a curved trajectory. The curve can differ between countries and often resembles either a concave-shaped, Bell-shaped or convex-shaped curve, depending on the (limited) historical sources found. The 1960 CE per capita land use value is generally lower than for the present day since population numbers have exploded since World War II. Land use was, however, limited by the lack of technology and this restricted the maximum amount of land that subsistent farmers could handle. We first estimated land use per capita for each country, and by multiplying this with the total population, we computed the total areas for cropland and grazing.

Further specific input statistics on a subnational level were taken for some of the larger countries in the world, such as the USA (USDA, 2006), Canada (Urquhart and Buckley, 1965), Mexico (World Atlas of Agriculture, 1969), Argentina (Vazquez-Presedo, 1988), Brazil (N. Ramankutty, personal communication, 2001), India (Flint and Richards, 1991; Indiastat, 2009), China (China National Bureau of Statistics, 2008; Ge et al., 2008; He et al., 2012, 2013) and Australia (Australian Bureau of Statistics, 2001). Furthermore, other country-specific sources were used when available for specific information per country. The methodology has also been described in detail in Klein Goldewijk et al. (2011); see also Supplement A for country-specific land use data sets.

For a spatially explicit depiction of present land cover we used the ESA Land Cover consortium maps (ESA, 2016; Hollman et al., 2013). The consortium produced a time series of three global 300 m spatial resolution land cover data sets predominantly based on MERIS satellite data, representative for the 1998–2002 CE, 2003–2007 CE and 2008–2012 CE periods. To produce the satellite reference map of HYDE 3.2, the most recent epoch has been used, representing 2010 CE. The ESA classes are aggregated to 5 arcmin grid cell fractions consistent with the HYDE land mask. Cropland and grazing land are allocated to the grid using the various ESA land cover classes, which are used in two ways: classes are grouped according to their probability to contain cropland and pasture, and then allocation takes place accordingly. First, the procedure tries to allocate as much cropland (or pasture) to the land cover classes in the probability group 1 (allocation step 1). Then in the second and third rounds as much of the remaining land is allocated to probability groups 2 and 3 (allocation steps 2 and 3), and finally, in a fourth round, priority group 4 is used to allocate the remaining land. In most cases, FAO areas are already allocated in steps 1 or 2. Several classes are defined to never contain cropland (or pasture). Additionally, we define the fraction of an ESA land cover class that is actually covered by cropland and pasture (numbers in Table 1): on cropland and grassland land cover types this is assumed to be 90 % to account for small areas of infrastructure, wetlands, unsuitable terrain, steep slopes or small patches of vegetation that are not explicitly identified in the original land cover product (Verburg et al., 2009). The mosaic cropland land cover types are defined to have 60 and 40 % of cropland or pasture following the managed grass definition of Poulter et al. (2015). First, cropland is allocated, then grazing land.

The allocation procedure first allocates FAO cropland areas to land cover types dominated by cropland (see probability group 1 in Table 1). Within the area that can be allocated a preference is given to cropland locations from the unified cropland layer map (Waldner et al., 2016). This is done in order to make use of the high-quality empirical data that are available and to correct for the characteristic that the ESA cropland land cover types are most likely a mix of cropland and pasture lands in many regions. If the land cover types dominated by cropland (probability group 1) do not cover sufficient area to allocate all FAO cropland area, land cover areas within the second category (shrubland cover, open forest or grassland) are allocated. If these areas are also insufficient, cropland is allocated to sparse vegetation, finally followed by bare lands. Priority is always given to cropland locations from the unified cropland layer map.

A similar approach is used to allocate grazing land in each country, following an almost identical order of allocation (see Table 1). In addition to a preferred allocation to the land cover types dominated by cropland, which were also used to allocate cropland; grazing land is also preferably allocated to the grassland land cover type. Cropland is given priority over grazing land and allocated before grassland, and thus the cropland that was allocated in the previous step reduces the area available for pasture. In addition, various region-specific rules are implemented. First, in Canada, Russia and the USA, various subnational regions known to have very little to no pasture area are excluded from allocation, e.g. inaccessible tundra areas. Second, in countries with substantial grazing land that can be allocated in large homogeneous areas (e.g. the Sahara) a preference is given to locations in close proxim-

Table 1. Percentages of cropland and grazing land allocated in four steps from the original ESA CCI land cover classes (between 0 and 100 %).

LCCS Class	UNLCCS land cover class description	Cropland		Pasture	
		A	B	C	B
10	Cropland, rain-fed	90	1	90	1
11	Herbaceous cover	90	1	90	1
12	Tree or shrub cover	90	1	90	1
20	Cropland, irrigated or post-flooding	90	1	90	1
30	Mosaic cropland (> 50 %)/natural vegetation (tree, shrub, herbaceous)	60	1	60	1
40	Mosaic natural vegetation (tree, shrub, herbaceous cover) (> 50 %)	40	1	40	1
50	Tree cover, broadleaved, evergreen, closed to open (> 15 %)	–	–	–	–
60	Tree cover, broadleaved, deciduous, closed to open (> 15 %)	–	–	–	–
61	Tree cover, broadleaved, deciduous, closed (> 40 %)	–	–	–	–
62	Tree cover, broadleaved, deciduous, open (15–40 %)	30	2	30	2
70	Tree cover, needleleaf, evergreen, closed to open (> 15 %)	–	–	–	–
71	Tree cover, needleleaf, evergreen, closed (> 40 %)	–	–	–	–
72	Tree cover, needleleaf, evergreen, open (15–40 %)	30	2	30	2
80	Tree cover, needleleaf, deciduous, closed to open (> 15 %)	–	–	–	–
81	Tree cover, needleleaf, deciduous, closed (> 40 %)	–	–	–	–
82	Tree cover, needleleaf, deciduous, open (15–40 %)	30	2	30	2
90	Tree cover, mixed leaf type (broadleaved and needleleaf)	–	–	–	–
100	Mosaic tree and shrub (> 50 %)/herbaceous cover (> 50 %)	40	2	40	2
110	Mosaic herbaceous cover (> 50 %)/tree and shrub (> 50 %)	60	2	60	2
120	Shrubland	90	2	90	2
121	Evergreen shrubland	90	2	90	2
122	Deciduous shrubland	90	2	90	2
130	Grassland	90	2	90	1
140	Lichens and mosses	–	–	–	–
150	Sparse vegetation (tree, shrub, herbaceous cover) (< 15 %)	90	3	–	3
152	Sparse shrub (< 15 %)	90	3	–	3
153	Sparse herbaceous cover (< 15 %)	90	3	–	3
160	Tree cover, flooded, fresh or brackish water	–	–	–	–
170	Tree cover, flooded, saline water	–	–	–	–
180	Shrub or herbaceous cover, flooded, fresh/saline/brackish water	–	–	90	3
190	Urban areas	–	–	–	–
200	Bare areas	90	4	90	4
201	Consolidated bare areas	90	4	90	4
202	Unconsolidated bare areas	90	4	90	4
210	Water bodies	–	–	–	–
220	Permanent snow and ice	–	–	–	–

A: fraction available for cropland. B: allocation step. C: fraction available for grazing land.

ity to previously allocated grazing area. The resulting maps for current cropland and grazing land are used as reference maps Wcrop_satellite and Wgrazing_satellite in the HYDE allocation procedure (see Sect. 3.2)

2.3.2 Rice

Total rice area statistics per country were taken from FAO for the post-1960 CE period. For the pre-1960 CE period, data for some rice-growing countries were taken from Mitchell (2007a, b, c) for the 1890–1950 CE period. The rest were hindcasted on a per capita basis for countries for which no historical data could be found. Global totals were compared with literature where possible to tune the per capita numbers. A correction was made for harvested area versus physical area. In China, for example this ratio of physical area to harvested area is around 0.6 due to multiple and triple cropping (Frolking et al., 2002), in Bangladesh 0.67 in 1980 CE and 0.55 in 2010 CE (Ara et al., 2016), in Vietnam 0.63 (range 1.25–0.48) (Wiens, 1998), and India 0.71–0.73 (GYGA, 2017; Kalaiselvi and Sundar, 2011). The 0.6 ratio was also applied to other Asian rice-producing countries; the rest of the world is assumed to have a ratio of 1.0. Ricepedia (2015) presents estimates for the fraction of rice that is irrigated per country for the present, and an assump-

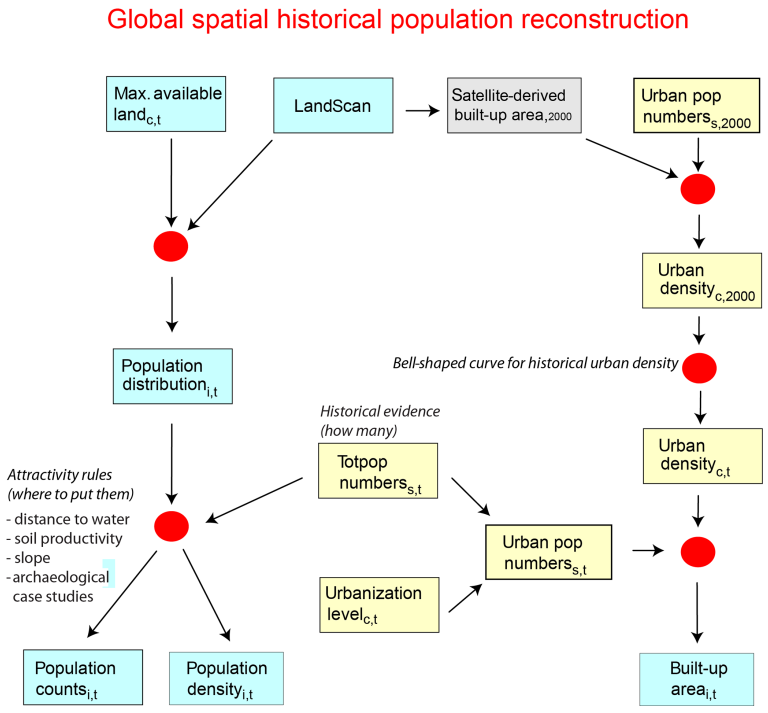

Figure 1. Population allocation scheme.

tion was made for that fraction at the start of agriculture. For the years in between, data were linearly interpolated towards the 2010 CE value (see Table S1 in the Supplement, "faostat_rice" sheet, columns CN : FM). In general, most arid regions were assumed to be irrigated, others rain-fed. Thus, for each time step the total amount of rice could be computed. Rain-fed rice was allocated first (most cost effective), irrigated rice second. The reference maps for rice were derived from MAP SPAM (You et al., 2014) and are used for the allocation for the present. They gradually change into combined weighting maps of the HYDE rules; see Sect. 3.

2.3.3 Irrigation

The input data for the category "areas equipped for irrigation" for the post-1960 CE period were taken from FAO (2015) and for the 1900–1960 CE period from Siebert et al. (2015). For the 1700–1900 CE period estimates were taken from Siebert (2008). For the pre-1700 CE period a per capita estimate was used to match global estimates of irrigated area found in literature. The statistics for the actual irrigated area for the 1960–2010 CE period were derived by multiplying FAO's category "area equipped for irrigation" with the fraction of "equipped/actual irrigated area" from the GMIA_v5 database of Siebert et al. (2015). For many countries this fraction is 1.0, but not for all countries. Therefore, we used the last known ratio and applied this to the complete series of "areas equipped for irrigation" to compute the historical time series of "actual irrigated area" (see Table S2). For the spatial representation of current global areas equipped for irrigation and actual irrigated areas, we used the Siebert et al. (2015) global data set of monthly irrigated and rain-fed crop areas around the year 2000 (MIRCA2000).

3 The HYDE allocation of population and land use

3.1 Allocation of population and built-up area

For the present, the spatial patterns from LandScan (2014) are used in our weighting maps to allocate our total population for each administrative unit. These patterns are gradually replaced with combined weighting maps based on various proxies such as soil suitability, slope, distance to water and case studies from several disciplines (e.g. history, archaeology) when going back in time (Fig. 1). Built-up areas (Uarea) are computed by dividing total urban population in a country at time t by average urban densities in a country at time t. These curves are computed per country and are assumed to follow a Bell-shaped curve trajectory, a specific pattern for increase and decrease in urban density in cities and towns over time but on different scales in various regions. See Fig. 1 and for a full description of the methodology Klein Goldewijk et al. (2010) and for the built-up area curve Supplement B.

3.2 Allocation of land use

3.2.1 Non-usable areas

We excluded specific areas from allocation. Protected areas as derived from the database of protected areas from the United Nations Environment World Conservation Monitoring Centre (UNEP/WCMC, 2013) were excluded from agricultural use. However, as protected areas were only established relatively recently, they are only excluded after 1900 CE until present. Before 1900 CE, they are potentially available for agriculture, but due to the tendency of the allocation model to not shift, keeping the location of agricultural areas when moving back in time, and due to their often low accessibility, these areas are not likely to be used before 1900 CE. Additionally, so-called "non-used areas" in Australia were excluded from the allocation of agriculture, based on a map from the Australian National Land and Water Resources Audit (NLWRA, 2001).

3.2.2 Allocation of land use

The order of allocation is as follows: first, we allocate cropland, then rice, then irrigation and finally grazing land.

Cropland

The method to allocate historical cropland is followed for each grid cell of 5′ by 5′ (ca. 85 km^2 around the Equator). The maximum area of a grid cell that is available for allocation of cropland ($\mathrm{Garea_{max}}$) is calculated as follows:

$$\mathrm{Garea_{max}} = [\mathrm{Garea_{cell}} - \mathrm{Uarea}_t - \mathrm{Parea}_t - \mathrm{NLarea}_t], \quad (1)$$

where $\mathrm{Garea_{cell}}$ is the land area of a 5′ grid cell (spherical Earth) except water bodies, snow and ice; Uarea_t is the urban built-up area for year t; Parea_t is protected area, but only valid for the post-1900 period (they did not exist before); and NLarea is the no-land-use area in central Australia (see Table S3 for the original input data and Fig. 2 for the cropland allocation scheme).

The land use statistics are allocated to grid cells according to a mix of two weighting maps: a reference map of 2010 CE for cropland ($\mathrm{Wcrop\_satellite_{2010}}$), derived from satellite imagery of ESA (2016) for the present (Eq. 2), and a historical map ($\mathrm{Wcrop\_historic}_t$) that is constructed on the basis of the six rules as described in the next section (Eq. 3).

$$\mathrm{Wcrop\_reference}_t = \mathrm{Wcrop\_satellite_{2010}} \quad (2)$$

For allocating historical cropland, six major assumptions were made. (i) Urban built-up areas (Uarea) were excluded for allocation (see Eq. 1). (ii) A population density (Wpopd) less than 0.1 cap km^{-2} does not allow permanent agriculture. (iii) Areas with better soil suitability according to the Global Agro-Ecological Zones map (GAEZ, 2000) FAO IIASA are used first (Wsuit). (iv) Easily accessible areas such as coastlines and river plains derived from Natural Earth (2015) are more promising for early settlement (Wcoast and Wriver). (v) Inaccessible terrains with steep slopes derived from NOAA-NGDC 5-Minute Gridded Global Relief Data (ETOPO5, 2005) are less promising for settlement (Wslope). (vi) Below an annual mean temperature of 0 °C no agriculture is possible (Wtemp_crop). The temperature map is derived from the Climate Research Unit (CRU) database of the University of East Anglia, UK, as an average for the 1960–1990 period (New et al., 1997). We normalized all weighting maps of these assumptions between 0 and 1 and multiplied them into a final, unique weighting map for each time step. This methodology is similar to the one already described in Klein Goldewijk et al. (2011).

$$\mathrm{Wcrop\_historic}_t = \mathrm{Wpop}_t \cdot \mathrm{Wsuit} \cdot \mathrm{Wriver} \cdot \mathrm{Wcoast} \cdot \mathrm{Wslope} \cdot \mathrm{Wtemp\_crop} \quad (3)$$

The final allocation is a combination of $\mathrm{Wcrop\_reference}_t$ and $\mathrm{Wcrop\_historic}_t$. We assume that the influence of $\mathrm{Wcrop\_reference}_t$ is zero in the year 1500 CE and 100 % in 2010 CE. Alternatively, the influence of $\mathrm{Wcrop\_historic}_t$ is zero in 2010 CE and 100 % in 1500 CE (and the pre-1500 CE period as well); see Supplement D for the technical description.

Rice

All rice-producing area is assumed to fall within the area defined earlier as cropland. For the spatial representation of global rice areas we used the International Food Policy Research Institute (IFPRI) Spatial Production Allocation Model (SPAM) maps from You et al. (2014). They present maps of the irrigated and rain-fed harvested area of rice.

Current reference maps for irrigated and rain-fed rice allocation:

$$\mathrm{Wir\_rice_{2010}} = \mathrm{Wir\_rice\_satellite_{2010}} \quad (4)$$

$$\mathrm{Wrf\_rice_{2010}} = \mathrm{Wrf\_rice\_satellite_{2010}}. \quad (5)$$

Extra weighting for the past is also determined by a historical geography map for rice-growing areas for the year 1000 CE (M. Widgren, personal communication, 2015). Also, the current reference maps for irrigated and rain-fed rice remain important for the allocation since the assumption is made that most rice-growing areas are very old, implying that current patterns are, to a great extent, representative for ancient patterns as well (see Table S4 for original input data and Fig. 2 for the cropland allocation scheme).

Historical weighting maps for rice allocation:

$$\mathrm{Wir\_rice}_t = \mathrm{Wrice_{1000}} \cdot \mathrm{Wir\_rice_{2010}} \quad (6)$$

$$\mathrm{Wrf\_rice}_t = \mathrm{Wrice_{1000}} \cdot \mathrm{Wrf\_rice_{2010}}. \quad (7)$$

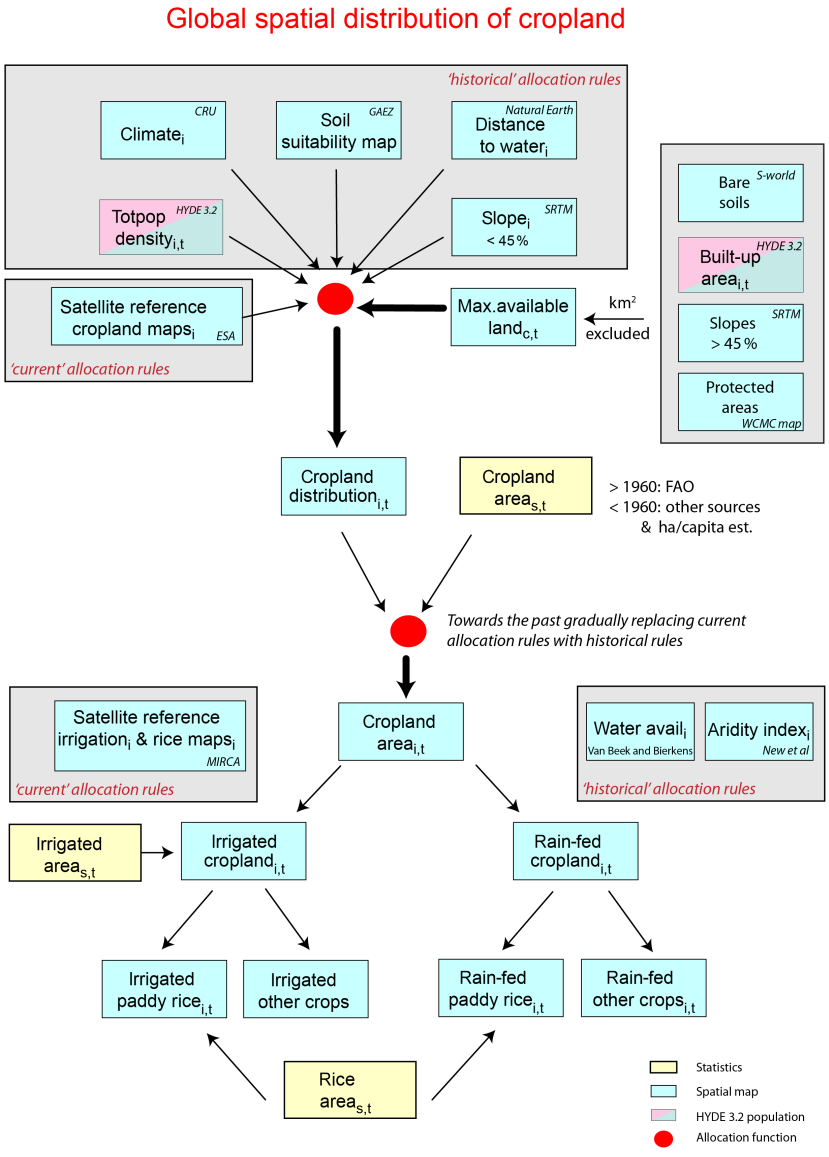

Figure 2. Cropland allocation scheme.

Irrigated area

The allocation of irrigated areas is comparable with that of cropland. First we use the reference map for 2000 CE for irrigated areas derived from the MIRCA (monthly irrigated and rainfed crop areas around the year 2000) database (Siebert et al., 2015). When hindcasting, we apply the HYDE rules for allocation based on the following assumptions. All irrigated area must fall within the computed cropland area. Next, we check whether there is enough water available to irrigate (Wwav), for which we use, as a proxy, a discharge map derived from Van Beek and Bierkens (2008). Furthermore, we assume that when the aridity index (Waridity) is low, the need for irrigation is higher. The aridity index is computed as annual precipitation divided by annual evapotranspiration, both derived from New et al. (1997). See Table S5 for original input data and Fig. 2 for the allocation scheme.

Current reference map for irrigated land allocation:

$$\mathrm{Wirri}_{2010} = \mathrm{Wirri\_satellite}_{2010}. \quad (8)$$

Historical weighting maps for irrigated land allocation:

$$\mathrm{Wirri}_t = \mathrm{Waridity} \cdot \mathrm{Wwav} \cdot \mathrm{Wirri}_{2010}. \quad (9)$$

Grazing land

As described above (Sect. 2.3), we define grazing land as land used for mowing or grazing livestock, based on the FAO category "permanent meadows and pastures". Grazing land can be a variety of ecosystems, ranging from managed irrigated grasslands to unmanaged open savannah woodlands

to semi-shrub/scrub, almost desert, lands. The method to allocate grazing land (to $\text{Garea}_{\text{max}}$ minus the already allocated built-up and cropland area) is comparable to the procedure for cropland. Natural grassland ecosystems as computed by the BIOME model were supplementary to the weighting maps. Biomes are a combination of plant functional types, defined by climatic variables and soil properties; see Prentice et al. (1992). Natural grasslands are assumed to be more attractive for use of grazing then other types (Wbiome); areas with a higher net primary production are also more favourable for grazing (Wnpp), and grazing is assumed to be impossible at annual average temperatures below $-10\,^{\circ}$C (Wtemp_grazing).

Current reference map for grazing land allocation:

$$\text{Wgrazing}_{2010} = \text{Wgrazing\_satellite}_{2010}. \quad (10)$$

We multiply the historical weighting maps for grazing land allocation:

$$\text{Wgrazing}_t = \text{Wpopd}_t \cdot \text{Wbiome} \cdot \text{Wnpp} \cdot \text{Wtemp\_grazing}. \quad (11)$$

See Table S6 for original input data and Fig. 3 for the grazing land allocation scheme.

Disaggregating grazing land into pasture and rangeland

For grazing lands, a distinction is made between more intensively managed pasture and extensively managed rangelands. The main difference between these two types of grassland is that rangelands comprise natural grasslands, shrublands, woodlands, wetlands, and deserts and grow primarily native vegetation, rather than plants established by humans, and typically have low livestock densities. The distinction, however, is often less straightforward, and transitions between the two forms exist in both time and space. To distinguish between these types of grasslands in a simple and transparent way, also historically, we apply – based on expert judgement – a population density and an aridity index, as low animal densities can be related to low population density, or to low productivity of the natural vegetation, which is approximated via the aridity index. When the aridity index (defined as annual precipitation divided by annual evapotranspiration) of a grid cell defined as grazing land is less than 0.5, or when the aridity index is higher than 0.5 but the population density is less than 5 inhabitants km^{-2}, then it is defined as rangeland.

Whether or not natural vegetation has been converted to establish grazing land is a very relevant question for studying the impacts of land use change. While most rangelands occur on land with mostly natural vegetation, low-intensity livestock grazing is also located in former forest or woodland areas, e.g. in Brazil. Therefore, after consultation with the Land Use Model Intercomparison Project (LUMIP), we recommend that our maps of pasture and rangeland be used for modelling purposes in the following way: for pastures, all natural vegetation is cleared and replaced by grass species. For rangeland, the natural vegetation remains intact if it is non-forest, but is cleared if it is forest. HYDE includes this distinction by providing two types of rangeland: (1) rangeland-natural is located in non-forest biomes (terrestrial ecoregions; Olson et al., 2001) and is therefore assumed not to have undergone conversion of natural vegetation. (2) Rangeland-converted is located in forest biomes (terrestrial ecoregions; Olson et al., 2001) and is assumed to have undergone conversion of natural vegetation. We also test this simple method against a more advanced, satellite-based approach to distinguish pasture and rangeland for the present day and find mostly a good agreement, except for some areas in Africa and central Brazil (see Supplement C).

4 Results

4.1 Population

We have constructed historical population maps for a 12 000-year period at a 5′ by 5′ grid resolution. Population numbers were very low at the start of the Neolithic era. We estimate 4.4 million in 10 000 BCE, which is in line with ranges of 1–20 million found in literature, with most estimates below 6 million; see also Klein Goldewijk et al. (2010) and Fig. 4. Our world population estimate for 5000 BCE is 19 million, in range with values between 5 and 20 million found in literature (Klein Goldewijk et al., 2010). Furthermore, we also estimate a lower estimate of 2 million and an upper estimate of 36 million in 5000 BCE (see Sect. 5). These lower and upper population estimates are eventually multiplied with the lower and upper per capita land use estimates to illustrate the bandwidth of uncertainty around our best estimate. It shows that especially for the pre-1700 CE period we have been very cautious in determining the lower and upper estimates, often outside the literature estimates, in order to capture any possible (extreme) population scenario in the past. We further estimate a global population in 1 CE of 232 million people (literature range 170–330 million, our uncertainty range 58–406 million).

Demographic and socioeconomic changes such as the rise and fall of the Egyptian, Greek, Roman, Indian, Chinese and American empires led to a global population estimate of 253 million in 500 CE (literature estimate 190 million, our range 101–406) and 323 million in 1000 CE (literature range 253–345, our range 176–568). The Columbian Exchange was the onset of true globalization. Shortly after Columbus landed in the Americas, the Industrial Revolution fuelled by colonization by Europeans of the Americas, Australia and later Africa, accompanied by a huge agricultural expansion, in the temperate regions and a bit later in the tropics as well. After 1700 CE, population growth accelerated, with an estimate of 592 million people in 1700 CE (literature range 410–680, our range 444–740), 943 million in 1800 CE (literature range 890–1000, our range 802–1086), 1643 million in 1900 CE (literature range 1571–1710, our range 1561–1725), 2531

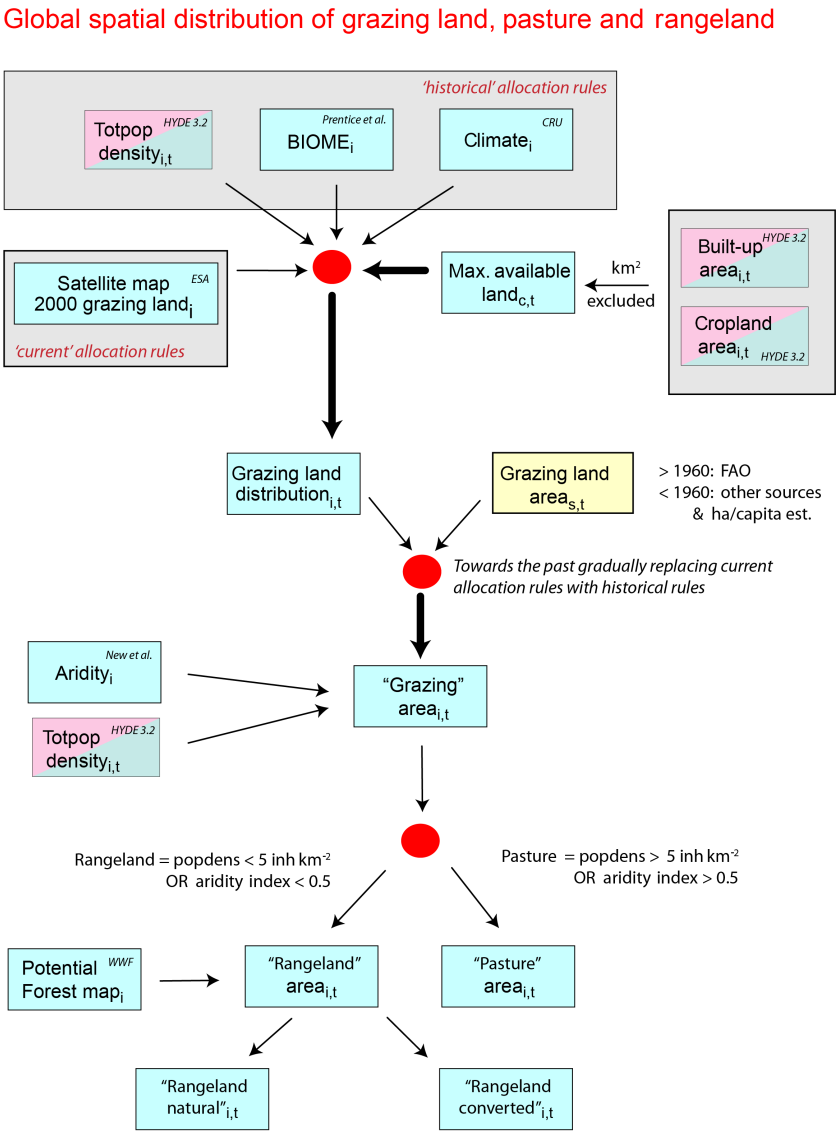

Figure 3. Grazing land allocation scheme.

million in 1950 CE, 4489 million in 1980 CE, 6113 million in 2000 CE and 7260 million in 2015 CE (see Table S7). The area occupied by built-up area (housing, building, etc.) is still very modest compared to the total land surface available: less than 0.10 % in 1900 CE and still less than 0.5 % in 2015 CE .

4.2 Croplands

Agriculture developed very slowly at the start of the Holocene after the domestication of plants and animals, in place as well as over time. We estimate the corresponding global cropland area extent in 5000 BCE at a very modest 6 million ha (range 1–18), which corresponds to 0.31 ha cropland cap^{-1} (range 0.05–0.57). Technology was limited and agriculture was dependent on local climate (environment) conditions. Agriculture was more prevalent throughout the Mediterranean, northern India and in eastern China during Greek and Roman times, most likely due to the existence of highly developed irrigation schemes. We estimate the global cropland area to reach 146 million ha at 1 CE (range 50–344), corresponding to 0.63 ha cropland cap^{-1} (range 0.16–1.10); see also Fig. 4.

The cropland area in 500 CE is estimated to be 133 Mha (67–269), 140 Mha (82–251) in 800 CE, 209 Mha (124–309) in 1100 CE and 219 Mha (148–299) in 1400 CE, which translates globally to around the same number of 0.50 (0.20–0.84) ha cropland cap^{-1} over that period because of population fluctuations. Our cropland estimate of 140 Mha for 800 CE is somewhat higher than the 136 Mha (range 80–220) of Pongratz et al. (2008) and close to their 197 Mha estimate

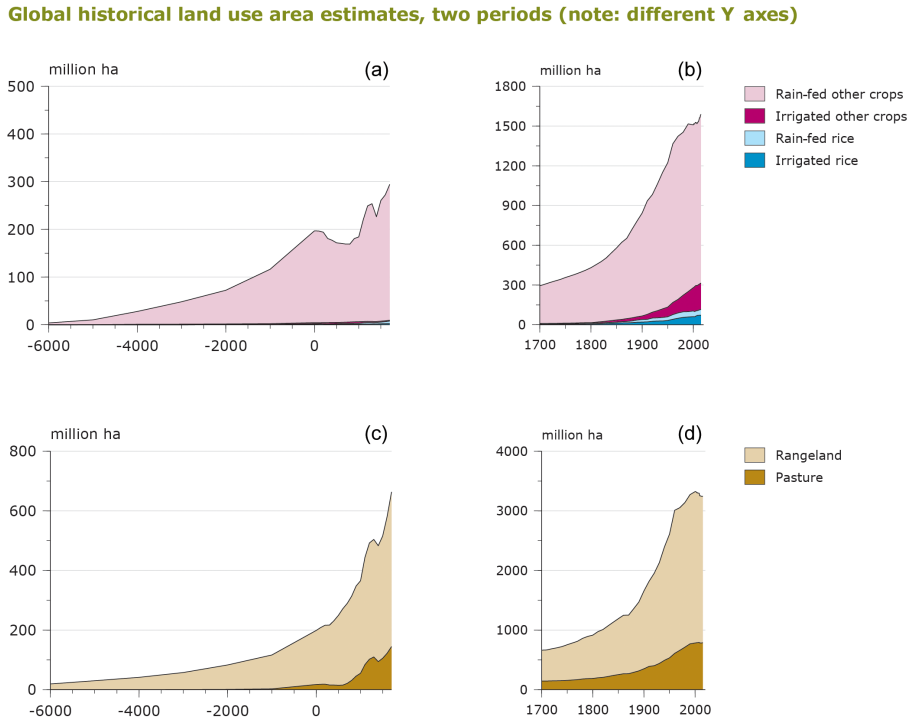

Figure 4. Summary of historical land use area estimates for different time periods. Cropland area for 6000 BCE–1700 CE **(a)** and 1700–2010 CE **(b)**. Grazing land area for 6000 BCE–1700 CE **(c)** and 1700–2010 CE **(d)**.

for 1100 CE but slightly lower than the 233 Mha for 1400 CE (see Tables 2 and S7).

As result of large population growth and technological developments, the total global area of cropland has doubled at a rapid pace since the 16th century from 293 Mha in 1700 CE to 578 Mha in 1850 CE, 1223 Mha in 1950 CE, 1532 Mha in 2000 CE and 1593 Mha in 2015 CE. The increase in global cropland area appears to have levelled off during the early 2000s but recently we have see an increase again. Ramankutty and Foley (1999) and Pongratz et al. (2008) estimated a value of around 400 Mha for 1700 CE. The latter can probably be explained by the fact that their hindcasting starting point in 1990 CE was already higher than that of the FAO because they also used non-FAO data (Pongratz et al., 2008); see Table 2.

Globally, the area of cropland per person increased slowly to a maximum of 0.8 ha cap^{-1} until 3000 BCE. Then it slowly decreased again to less than 0.5 ha cap^{-1} at the end of the 18th century, with a small temporary increase to 0.53 ha cap^{-1} in the early 20th century. However, after 1950 CE it decreased again to 0.22 ha cap^{-1} in 2015 CE due to the strong population growth. Apparently, technology alone could not compensate entirely for the explosive population growth after World War II, and since the best soils are already occupied, this trend will continue.

4.3 Irrigated land

Irrigation played a vital role in the existence and spread of agriculture. In general, irrigation can be defined as applying additional water (in addition to natural rainfall) to the soil in order to enhance crop yield. First, surface water was diverted from lakes, streams and rivers to other places in the landscape. Later, various types of pumps were used, driven by either livestock (oxen, mules, horses), manpower or, eventually, machines. The earliest archaeological evidence for irrigation can be dated to around 6000 BCE in Jordan and Egypt (Sojka et al., 2002). In the millennia that followed, irrigation was diffused across the Levant region and the Mediterranean. At the same time, irrigation emerged independently in India, Pakistan and China. In addition, in the Americas the Inca, Maya and Aztec already had irrigation schemes in the first millennium. A little later in time, the Hohokam practiced irrigation in the dry southwestern USA only to disappear mysteriously in the 14th century (Sojka et al., 2002). We estimate the global irrigated area to be less than 0.2 Mha in 5000 BCE, 2.6 million ha in 1 CE, very slowly increasing to 4.1 Mha in 1000 CE and levelling off at 4.2 Mha in 1500 CE; see Table 3.

The 19th century marked a significant change in technology in many areas of science. Ancient irrigation technology worked properly in already favourable environmental conditions (rainfall, terrain, slope), but when population grew and agriculture expanded into areas with less favourable conditions, things had to change. Electrical, steam and internal

Table 2. Regional cropland area estimates (million ha).

Regional cropland area estimates (million ha)																	
	4000 BCE	3000 BCE	2000 BCE	1000 BCE	1 CE	800 CE	1100 CE	1400 CE	1700 CE	1800 CE	1850 CE	1900 CE	1920 CE	1950 CE	1960 CE	2000 CE	2015 CE
North America	0.0	0.0	0.0	0.2	0.4	0.6	0.8	1.1	0.8	8.3	44	153	199	232	237	230	208
Latin America	1.1	3.8	5.3	6.1	6.9	11.1	15.2	19.5	9.0	16.0	20	32	51	84	101	161	198
Europe	1.0	3.3	7.2	14.4	33.6	26.9	43.1	50.2	78.0	100.7	123	148	151	155	157	136	127
USSR	0.5	1.4	1.6	2.8	3.1	5.3	8.3	12.0	21.6	46.9	70	130	154	196	235	212	204
N.Africa_M.East	13.4	16.4	16.9	20.8	25.4	23.6	21.3	18.0	21.3	24.0	32	41	46	63	78	87	86
Tropical Africa	0.3	1.2	1.9	2.8	4.4	13.8	19.4	27.1	39.1	42.2	48	61	70	112	144	202	249
China	2.7	6.0	12.2	24.1	47.8	24.4	61.5	46.9	62.3	80.7	89	94	103	110	110	133	128
South Asia	1.5	3.6	6.4	11.3	21.6	30.4	33.9	36.7	49.6	94.8	132	143	149	185	210	220	222
SE Asia	0.1	0.5	0.7	1.1	1.7	3.7	4.9	7.1	11.6	15.3	18	34	47	62	73	100	120
Pacific dev.	0.0	0.0	0.0	0.0	0.0	0.0	0.0	0.0	0.0	0.1	0.3	4.3	10	24	34	50	50
World	21	36	52	84	145	140	209	219	293	429	20	840	51	1223	1377	1531	1591
– lower estimate	5	9	14	26	48	80	124	148	220	366	522	800	940	1186	1342	1512	1572
– upper estimate	49	84	123	197	333	251	309	299	367	494	637	884	1022	1259	1413	1542	1604
Other global estimates																	
Houghton et al. (1983)									264								
Esser (1991)												1390	1570	1910			
Richards (1990)									265		537		913	1170			
Ramankutty and Foley (1999)									405	678	821	1144	1301	1528	1688		
Klein Goldewijk (2001), HYDE 2.0									266	402	537	813	944	1230			
Pongratz et al. (2008)						136	197	233	401								
Klein Goldewijk (2001), HYDE 3.1					130				300	418	562	849	995	1214		1531	
FAO (2015)															1372	1519	1591

Table 3. Regional irrigated area estimates (million ha).

Regional actual irrigated area estimates (million ha)													
	4000 BCE	3000 BCE	2000 BCE	1000 BCE	1 CE	1000 CE	1500 CE	1700 CE	1800 CE	1900 CE	1960 CE	2000 CE	2015 CE
North America	0.00	0.00	0.00	0.00	0.00	0.0	0.0	0.0	0.0	3.2	15.7	22.6	22.1
Europe	0.00	0.00	0.00	0.03	0.11	0.2	0.4	0.1	0.3	2.2	5.8	14.9	21.4
USSR	0.00	0.00	0.00	0.00	0.03	0.1	0.1	0.2	0.3	2.9	7.0	12.0	11.4
Pacific dev.	0.00	0.01	0.01	0.01	0.05	0.1	0.2	0.3	0.7	3.2	6.4	13.2	13.2
China	0.86	0.99	1.05	1.14	1.28	1.9	1.0	0.9	0.9	2.8	10.1	20.7	23.8
Latin America	0.00	0.00	0.00	0.00	0.01	0.0	0.1	0.1	0.2	0.8	2.4	5.4	6.8
N.Africa_M.East	0.07	0.15	0.30	0.60	0.91	1.2	1.7	1.8	4.1	11.3	39.7	48.8	64.4
Tropical Africa	0.02	0.04	0.06	0.11	0.20	0.4	0.5	0.7	2.0	16.4	35.0	73.4	86.4
South Asia	0.00	0.00	0.00	0.00	0.00	0.1	0.2	0.4	0.8	4.6	10.4	20.2	23.8
SE Asia	0.00	0.00	0.00	0.00	0.00	0.0	0.0	0.0	0.0	0.1	0.7	1.8	2.4
World	0.95	1.19	1.42	1.90	2.61	4.1	4.2	4.5	9.3	47.5	133.2	233.0	275.6
Other global estimates													
Siebert (2008)								4.5	10.5	53.2		278.9	
Siebert et al. (2014)												255.2	
Framji et al. (1982)										40.0			
Michael (2008)										40.0			
Li et al. (2009)										50.0			
Siebert et al. (2015)										63.0	144.5	262.9	
Freydank and Siebert (2008)								5.1	10.6	53.2			
FAO (2015)											163.5	288.9	

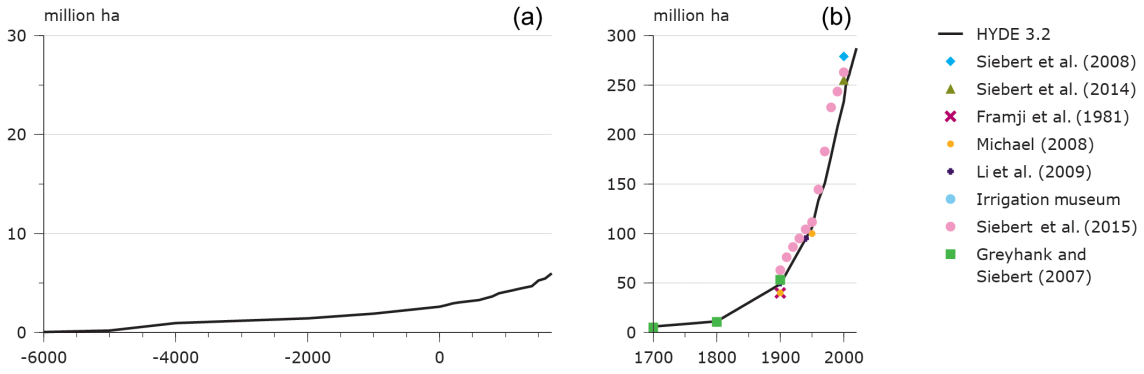

Figure 5. Historical (actual) irrigated area estimates for two periods: 6000 BCE–1700 CE **(a)** and 1700–2010 CE **(b)**.

combustion engines became available for pumping water – even in remote areas from large groundwater reservoirs many metres deep. This enabled farmers to grow crops where agriculture had previously not been possible; hence, the area in which irrigation was used increased on a large scale.

We estimate the global irrigated area in 1700 CE to be 4.5 Mha, which is similar to the estimate of Siebert (2008) and close to the 5.1 Mha of Freydank and Siebert (2008); see Fig. 5. Our estimate for 1800 CE of 9.3 Mha is close to the 10.5 Mha of Siebert (2008) and the 10.6 Mha of Freydank and Siebert (2008). In addition, our estimate of 48 Mha for 1900 CE is well within the literature range of 40–63 Mha (Framji et al., 1982; Freydank and Siebert, 2008; Li et al., 2009; Michael, 2008; Siebert, 2008; Siebert et al., 2015). Finally, we estimate the global irrigated area in 2015 CE at 276 Mha, with a large share in China (63 Mha) South Asia (88 Mha) and South East Asia (24 Mha).

4.4 Rice

Many studies agree that the origins of rice agriculture began in the lower Yangtze River valley in eastern China (Barker, 2006; Bellwood, 2001; Fuller et al., 2007; Zhang and Wang, 1998). These findings form the basis for the hypothesis that rice cultivation that led to domestication began in 6000 BCE. During the period from 6000 BCE until around 4000 BCE, systematic cultivation of rice species had become well established (Opferkuch, 2016).

We cautiously estimate rice area in China to be less than 0.0004 Mha in 8000 BCE, 0.03 Mha in 6000 BCE, 0.02 Mha in 4000 BCE, 0.11 Mha in 2000 BCE, 1 Mha in 1 CE and 1.2 Mha in 1000 CE (see Table 4). However, these numbers are highly uncertain and must be treated with care. Numbers for South East and South Asia show a similar pattern but that might be incorrect for the distant past (before 1 CE). Fuller and Qin (2011) suggest that rice arrived later in South East and South Asia and was fully domesticated around 4000 BCE. On a global scale, we estimate a rice area of 0.004 Mha in 8000 BCE, 0.02 Mha in 6000 BCE, 0.11 Mha in 4000 BCE, 0.49 Mha in 2000 BCE, 2.6 Mha in 1 CE and 4.8 Mha in 1000 CE. This is in good agreement with the study of Fuller et al. (2011), who estimated a total rice area of 0.10 Mha in 4000 BCE, 0.20 Mha in 3000 BCE, 0.50 Mha in 2000 BCE, 0.80 Mha in 1000 BCE and 2.50 Mha in 1 CE (see Table 4 and Fig. 6). We did not find any global rice area estimates for the 1000 CE–1900 CE period in literature.

4.5 Grazing land

We estimate grazing land in 5000 BCE to be around 30 million ha (range 5–58), corresponding to 1.58 ha cap^{-1} of grazing land (range 0.23–2.87). Grazing land is estimated to be 199 million ha (range 50–353) in 1 CE and 1.05 ha grazing land cap^{-1} (range 0.22–1.54). The area for grazing land was higher than for cropland, namely 314 Mha (range 155–526) in 800 CE, 444 Mha (range 260–645) in 1100 CE and 483 Mha (range 326–660) in 1400 CE, which corresponds globally to 1.10 ha of grazing land cap^{-1} and 1.12 and 1.09 ha cap^{-1}. Our grazing land estimates are, in general, higher than the Pongratz et al. (2008) estimates; they present 140 Mha for 800 CE (range 80–210), 198 Mha for 1100 CE and 227 Mha for 1400 CE (see Tables 5 and S7).

We compute a global area used for grazing of 664 Mha in 1700 CE, which is higher than the 526 Mha of Houghton et al. (1983). The largest differences appear to be in tropical Africa, but the largest differences could arise from the fact that we distinguish between pasture and rangeland (145 Mha of pasture and 519 Mha of rangeland in 1700 CE). The latter is assumed to only involve a conversion from natural ecosystem to grazing land if it is located on forest land, whereas Houghton by design wanted to exclude grasslands, which did not involve conversion of natural shrubs. In 1800 CE the area occupied for grazing had grown to 915 Mha (189 Mha pasture and 726 Mha rangeland), and 1657 Mha in 1900 CE (351 Mha pasture and 1306 Mha rangeland). The area of grazing land reached a peak around 2000 CE with 3322 Mha (784 Mha pasture and 2538 Mha rangeland) and has been slowly decreasing towards the present day. The largest increase in pastures appears to have occurred in the second half of the 20th century in tropical Africa, followed by Latin

Table 4. Regional rice area estimates (million ha).

Regional rice area estimates (million ha)													
	4000 BCE	3000 BCE	2000 BCE	1000 BCE	1 CE	1000 CE	1500 CE	1850 CE	1900 CE	1930 CE	1960 CE	2000 CE	2015 CE
North America	0.00	0.00	0.00	0.00	0.00	0.00	0.00	0.00	0.15	0.39	0.86	1.23	0.88
Latin America	0.00	0.00	0.00	0.00	0.00	0.00	0.00	0.10	0.40	1.14	6.19	6.40	5.36
Europe	0.00	0.00	0.00	0.00	0.00	0.03	0.06	0.17	0.28	0.30	0.39	0.43	0.47
USSR	0.00	0.00	0.00	0.00	0.00	0.02	0.04	0.16	0.22	0.27	0.33	0.51	0.43
N.Africa_M.East	0.00	0.00	0.01	0.02	0.07	0.13	0.14	0.30	0.34	0.49	1.04	1.36	1.33
Tropical Africa	0.00	0.00	0.00	0.00	0.00	0.09	0.42	1.14	1.33	1.71	3.20	7.05	11.46
China	0.02	0.05	0.11	0.16	1.00	1.18	3.19	16.22	15.39	19.33	21.08	20.51	20.78
South Asia	0.08	0.16	0.31	0.60	1.18	1.95	2.35	4.65	10.26	13.30	36.79	42.19	42.84
SE Asia	0.01	0.02	0.06	0.15	0.36	1.40	2.49	5.64	12.13	18.99	23.91	30.06	34.57
Pacific dev.	0.00	0.00	0.00	0.00	0.00	0.00	0.00	0.00	0.01	0.01	0.04	0.15	0.17
World	0.11	0.22	0.49	0.93	2.62	4.80	8.70	28.38	40.50	55.94	93.83	109.89	118.29
Other global estimates													
Fuller et al. (2011), wet rice	0.05	0.20	0.40	0.70	2.30								
Fuller et al. (2011), total rice	0.10	0.20	0.50	0.80	2.50								
Barker et al. (1985), harvested are										81.3			
FAO (2015), harvested area											115.4	132.9	

FAO: area harvested. HYDE: standing crop area.

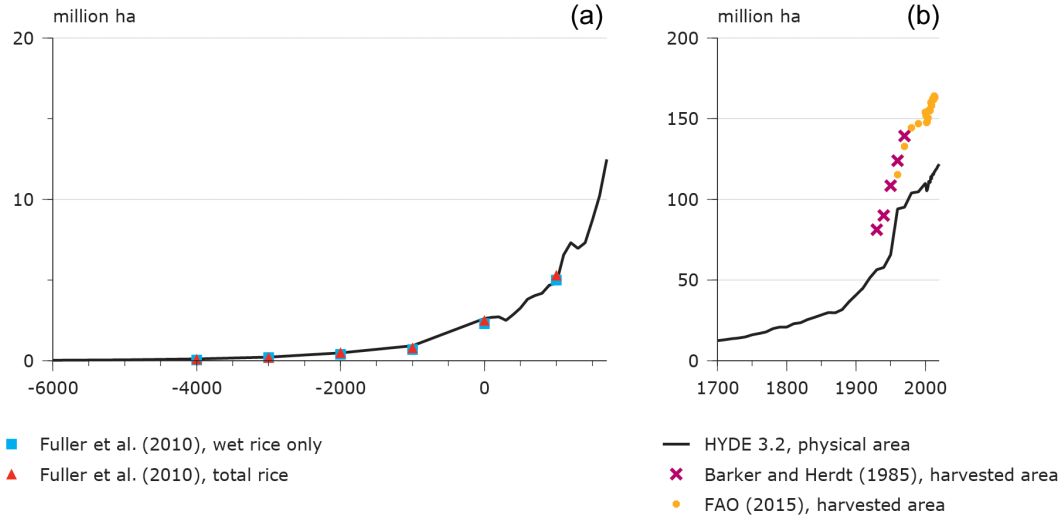

Figure 6. Historical (physical) rice area estimates for two periods: 6000 BCE–1700 CE **(a)** and 1700–2010 CE **(b)**.

America, and to a lesser extent in China. In North America and China, it seems to have stabilized in the last 10 to 20 years, while in Africa it is still increasing. Europe already had its peak around 1900 CE and is still declining slowly. Rangeland areas also increased in tropical Africa and Pacific developed countries (Japan, Australia, and New Zealand) up to World War II, but then declined slowly or stabilized at current levels.

Grazing land had a global low per capita average number of around 1.0 ha cap^{-1} until 1 CE, then a moderate increase to 1.13 ha cap^{-1} towards 1000 CE and then a gradually decrease again to 0.45 ha cap^{-1} in 2015 CE (see Table S7). However, regionally there are large differences. Sparsely populated countries such as Australia, Botswana, Mauritania and Namibia have more than 40 ha of grazing land per capita available today and Mongolia and Western Sahara even have around 150 ha cap^{-1}.

Table 5. Regional grazing land area estimates (million ha).

Regional grazing and area estimates (million ha)																	
	4000 BCE	3000 BCE	2000 BCE	1000 BCE	1 CE	800 CE	1100 CE	1400 CE	1700 CE	1800 CE	1850 CE	1900 CE	1920 CE	1950 CE	1960 CE	2000 CE	2015 CE
North America	0.0	0.0	0.0	0.0	0.0	0.0	0.0	0.0	4.2	18.2	36.1	158.0	181.3	278.1	280.8	251.8	266.7
Latin America	0.0	0.0	0.0	0.0	0.0	0.0	0.0	0.0	29.5	45.4	73.1	152.7	216.7	370.7	457.2	553.5	559.2
Europe	0.9	1.7	3.9	7.6	19.0	31.4	75.3	74.2	87.5	78.5	88.6	97.2	99.0	98.8	90.7	78.2	70.2
USSR	13.0	15.1	17.7	20.6	24.0	38.5	47.2	58.6	79.8	118.9	148.5	225.7	263.3	274.0	301.0	361.7	369.5
N.Africa_M.East	4.5	6.9	10.7	15.8	26.1	38.1	36.8	33.3	41.0	62.2	107.9	140.9	156.2	196.0	250.6	307.8	292.8
Tropical Africa	15.4	22.7	34.0	51.6	79.0	147.2	180.1	222.4	301.8	352.6	400.9	458.5	500.1	697.0	799.6	804.9	766.3
China	7.4	10.9	16.1	19.7	48.1	45.2	90.1	80.0	98.5	214.5	298.0	288.1	317.0	311.4	367.3	520.1	506.1
South Asia	0.0	0.1	0.3	0.6	1.4	10.4	11.0	9.8	13.2	16.1	18.8	24.8	28.1	38.6	51.7	49.1	48.5
SE Asia	0.2	0.2	0.5	0.9	1.2	2.9	3.3	4.4	7.1	7.1	8.0	12.5	15.5	18.3	17.3	17.2	17.5
Pacific dev.	0.0	0.0	0.0	0.0	0.0	0.0	0.0	0.2	1.2	1.4	11.6	98.8	175.5	328.2	393.5	378.3	344.6
World	41.4	57.7	83.1	116.6	198.8	313.8	443.8	483.0	663.5	914.9	1191.6	1657	1953	2611	3010	3323	3241
Other global estimates																	
Houghton et al. (1983)									526								
Pongratz et al. (2008)						144	198	227	370								
Klein Goldewijk (2001), HYDE 2.0									524	942	1310	1955	2282	2930			
Klein Goldewijk et al. (2011), HYDE 3.1					106				324	513	721	1294	1769	2464		3429	
FAO (2015)															3095	3424	3359

4.6 Regional trends

There are large differences in the land use history of the world's regions. Figure 7 depicts the land use development for selected time periods for the different world regions. Europe, the Middle East–North Africa–Turkey (MENAT), China and South Asia started agriculture much earlier than most other regions. North and Latin America and Oceania witnessed a relative late expansion of agriculture, but – once started – the expansion of cropland has been massive. In most regions, now and historically, cropland has been largely rain-fed, while South Asia, South East Asia and China have also had a significant share of irrigated crop area. The share of pasture in the total grazing land area is relatively high in Europe and South East Asia, while the share of rangeland is more dominant in North America, Latin America, the Middle East, the former USSR, tropical Africa and Pacific developed countries.

The share of irrigated land was very modest compared to the total amount of agricultural land for a long time. Only during the 20th century did this share increase, especially in South Asia and South East Asia.

Spatial patterns of agricultural land use are depicted in Fig. 8. The maps represent land use for the year 2010 for the different HYDE categories. Irrigated croplands are mainly concentrated in India, China, central Asia and North America. The main rain-fed cropland areas are more widespread all over the world in and concentrate in central and eastern North America, southeast Latin America, Europe, central Asia, sub-Saharan Africa, India, East and South East Asia, and the southwest and southeast parts of Australia. Irrigated rice is concentrated in eastern China, northern and eastern India, South East Asia, Japan, the Philippines, and Indonesia, while rain-fed rice can mostly be found in India, South East Asia, Madagascar, western Africa and Brazil.

The pasture areas are mostly located outside the arid regions such as the eastern USA, central America, eastern Brazil and Argentina, Europe, and the northern ranges of central Asia, sub-Saharan Africa, Madagascar, and eastern China. The rangelands can be found in the more arid and remote regions such as the western part of the USA and Mexico, southwest Brazil and the southern part of Argentina, the Sahel region of Africa, and the dry regions of southern Africa, North Africa, and the Arabian peninsula, the dryer parts of central Asia, Mongolia, and China, and the remote parts of Australia, except for the deep interior.

5 Uncertainties

There are large and many uncertainties that come with the hindcast methods applied in this study. We start with good and reliable data from the United Nations World Population Prospects for the post-1950 period, but before 1950 there is a strong dependency on a few historical population data sources such as McEvedy and Jones (1978), Madisson (2001) and Livi-Bacci (2007), which are for some regions and time periods not undisputed and probably on the low side of estimates (Klein Goldewijk and Verburg, 2013). Therefore, especially deeper into the past (pre-1500 CE), the numbers must be treated with caution. However, as already stated in Klein Goldewijk and Verburg (2013), the resulting demographic growth rates seem plausible, and thus the data are acceptable for the purpose of this study.

A similar statement can be made for the different land use estimates. The FAO data for post-1960 are quite reliable, al-

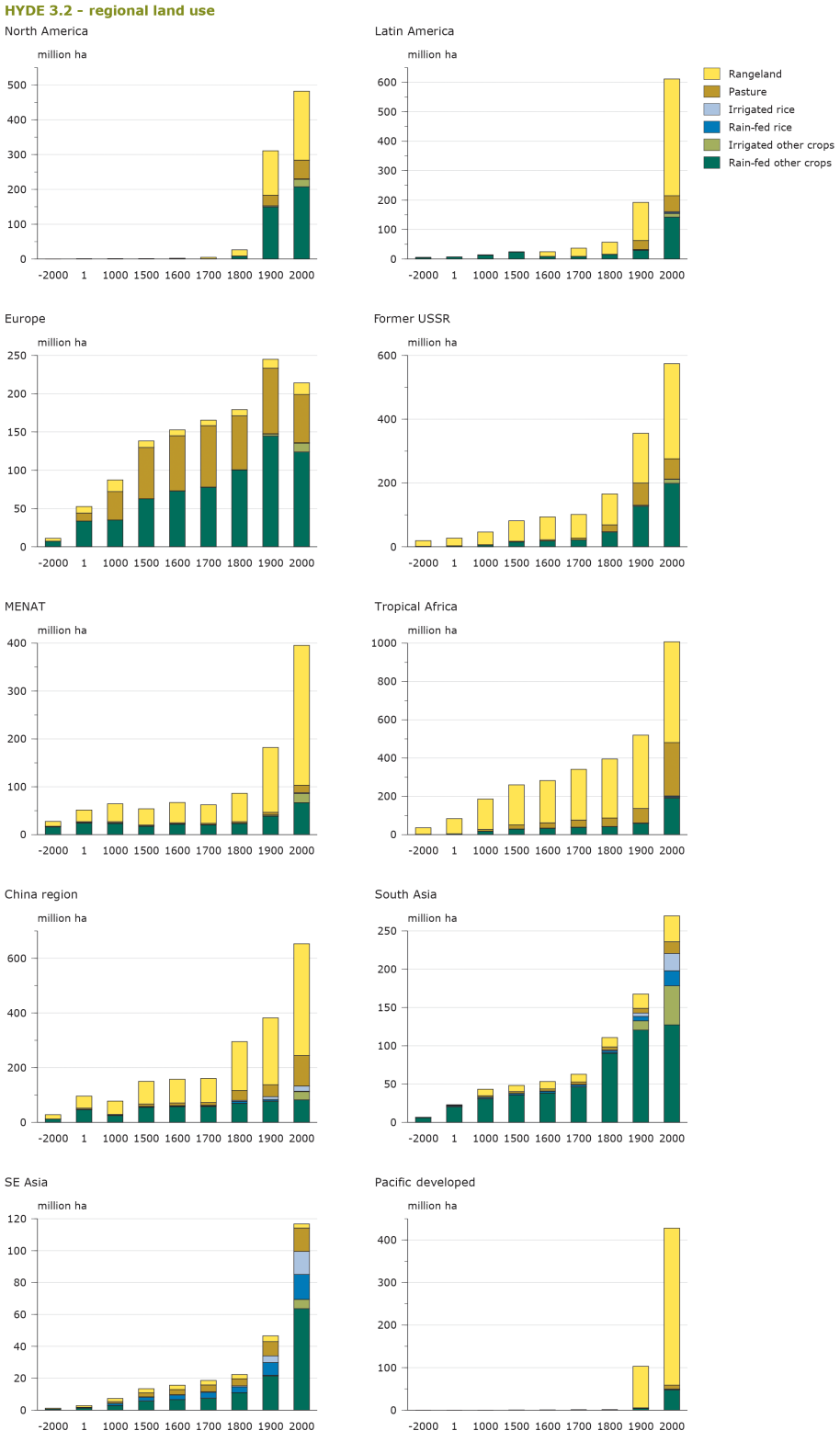

Figure 7. Historical land use estimates by region, for irrigated and rain-fed rice and other crops, rangeland and pasture. Please note the rangeland and pasture distinction is purely an indication of the intensity of use, not of the land use conversions involved (see Sect. 3.2.2 "Grazing land").

though for some countries they can be questioned, even for the present. The hindcasting approach of using land use per capita is a pragmatic approach, but it is very sensitive to the shape of the curve into the past. The minimum and maximum values per curve are very uncertain and vary substantially by country and in time. The study of Klein Goldewijk and Verburg (2013) clearly showed that the shape of the per capita curve profoundly determines the total agricultural area, especially in the pre-industrial era. Basic assumptions are that it is not zero, but there is also an absolute limit to the amount of work a person can do per day or year (Williams, 2000).

Making the distinction between pasture and rangeland is difficult and uncertain, also in the recent past, as this distinction is not covered by FAO statistics, though a distinction between permanent meadows and pastures into "cultivated" and "natural growing" is already available for some countries (FAOSTAT, 2017). We therefore applied a combined population density and aridity index to reflect livestock densities and an additional rule that pastures involve conversion of natural vegetation, while rangeland only involves conversion of natural vegetation if it was forest or woodland. The method has been compared to a more advanced approach and shows good agreement with satellite data (see Supplement C).

On top of the default estimates of population, cropland and grazing land, we also estimated lower and upper uncertainty ranges. These uncertainty ranges were partly based the ranges we could find in literature and partly on our own expert judgement and should be treated with care. The uncertainty range A is cautiously estimated at 1 % in 2000 CE, 5 % in 1900 CE, 10 % in 1800 CE, 25 % in 1700 CE, 50 % in 850 CE, 75 % in 1 CE and 95 % in 10 000 BCE. The uncertainty range B is twice the uncertainty range of A and should be considered as such since in our opinion it is highly unlikely that areas of cropland or grazing land have been outside this range in the past. The years in between were linearly interpolated (the method is similar to that described in Klein Goldewijk et al., 2010), and the resulting ranges are depicted in Fig. 8. A regional summary of cropland, pasture, population, per capita cropland area and per capita pasture area is presented in Table S7.

Figure 9a and b depict the range in total population estimates that we could find in literature and the HYDE baseline estimate (solid black line) for the period 10 000 BCE to 1700 CE (plate A) and 1700 CE to 2000 CE (plate B). The range in literature estimates for the last 300 years are not so large, meaning that apparently the uncertainty is consequently also rather small. This is also reflected in the range we applied to our own estimates, on top of the baseline, varying from 1 % in 2000 CE to 25 % in 1700 CE. Before 1700 CE the literature estimates show much more variation. For example, the lower literature estimate found for 1 CE is 27 % lower than our baseline estimate, while the upper estimate found in literature is 42 % higher than ours. Our range of plus and minus 75 % for 1 CE is therefore on the cautious side but expresses our idea that values outside our uncertainty bands are very unlikely to have occurred in the past. Figure 9c and d are the resulting total population estimates of HYDE, with their uncertainty bands A and B. Please note the different y axes. Figure 9e and f depict the HYDE baseline estimate of cropland with their uncertainties. Figure 9g and h show the HYDE estimates for grazing land.

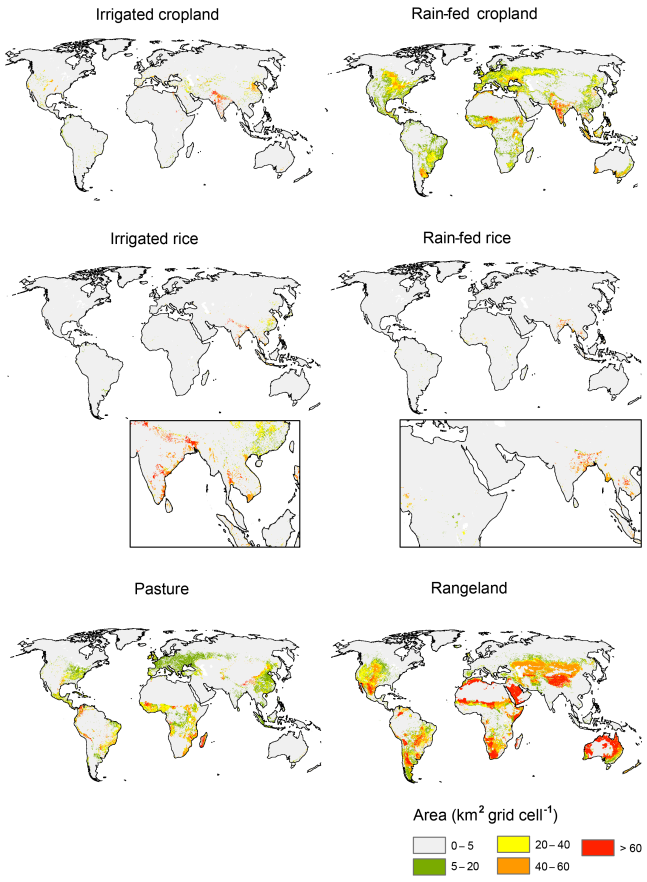

Figure 8. Spatial maps of cropland (irrigated and rain-fed), rice (irrigated and rain-fed), and pasture and rangeland for 2010 CE (six panels).

The final estimate of cropland and grazing land in HYDE is thus computed by multiplying population numbers and the per capita land use estimate for each scenario; a baseline, a first lower and upper estimate scenario (range A) and the second lower and upper estimate scenario (range B); see Fig. 9. The estimates for HYDE 3.2 are in general higher than the older estimates of HYDE 3.1. This is partly because of the use of new (census) data sources from the Clio Infra project (https://www.clio-infra.eu/), and partly because of new insights into long-term per capita land use (see also Klein Goldewijk et al., 2017). Especially grazing land has now been estimated to be much higher than before, reflecting that livestock grazing has been a long-term and widespread activity.

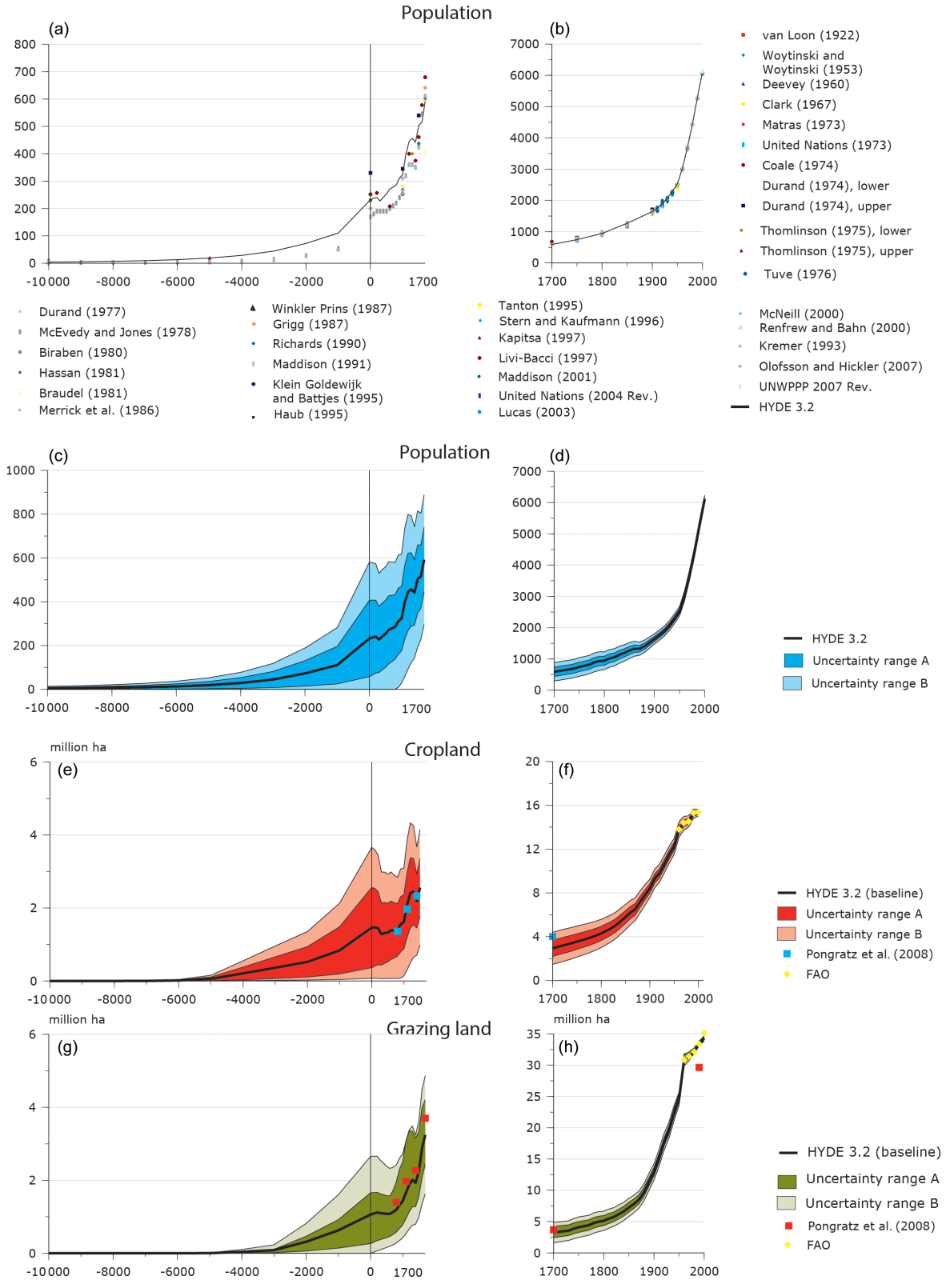

Figure 9. Available sources for population estimates **(a, b)**, and uncertainty ranges for global population **(c, d)**, cropland **(e, f)** and grazing land **(g, h)**, split into recent past (1700 CE onwards) and before 1700 CE to allow for different scales.

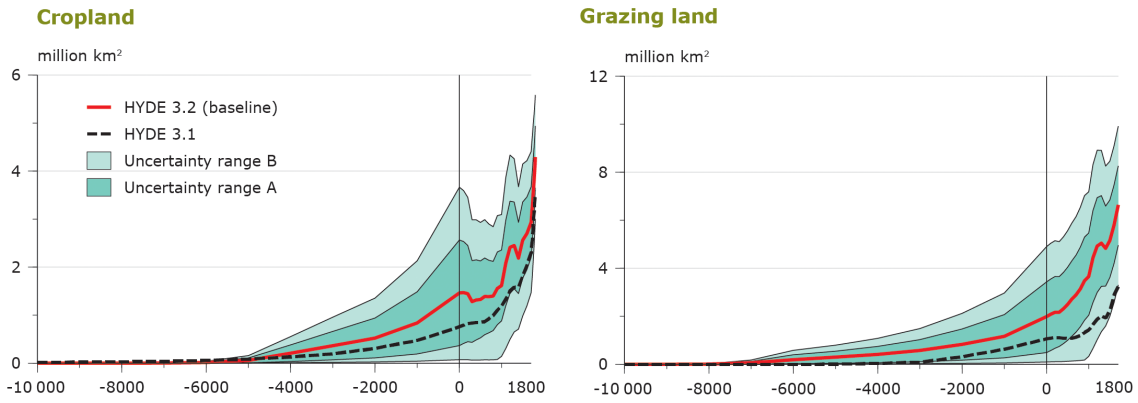

Figure 10. Comparison of HYDE 3.1 and HYDE 3.2, with uncertainty ranges.

We also quantified the amount of variation or dispersion in the input parameters in the per capita land use categories, used for computation of the total areas. Figure 10 depicts the results. The standard deviation (function STDEV.P in Excel) for cropland per capita remains around plus and minus 0.5 ha cap^{-1} for a long time. Only in the distant past, before 1 CE, does it increase to 1 ha cap^{-1}. The variation in the per capita grazing land values is much larger, up to 25 ha cap^{-1}, especially in the 18th and 19th centuries during the period of colonization. Before 1600 CE it is around 5 ha cap^{-1} (see Fig. 11).

The variation in irrigated land per capita is relatively high in recent years due to several irrigation projects worldwide. The peak in 4000 BCE is due to the high value for Egypt and some Middle Eastern countries. The per capita rice variation has been plus and minus 0.03 ha cap^{-1} (roughly around ±50 %) during the last decades, but then increases towards more than 100 % before 1960 CE (see Fig. 11).

Another issue is that due to the absence of transient Holocene climate and vegetation maps, we simplified things by using weighting maps for current climate and biome over the whole time period. Although the climate in 10 000 BCE differs from the present day (Armesto et al., 2009; Bertrand and Van Ypersele, 2002; Kropelin et al., 2008; Tett et al., 2005; Verschuren et al., 2002), we believe that the lower temperature thresholds we used are still valid, partially since they are just one of the factors involved. The same applies to the biome map. The Sahara desert was more like a grassland/savanna type during the pre-5000 BCE period (Verschuren et al., 2000) and changed into the current desert state later on, but it has been hardly populated (ample agriculture); thus, allocation procedure remained unchanged during that era.

Analysis by Prestele et al. (2016) show that it is quite crucial for future outcomes to determine at what spatial starting point global change models and integrated assessment models start their simulations. Therefore, we have also experimented with a different choice for the cropland and grazing land reference maps to see whether it would have an influence, and if so, to what extent the spatial patterns of land use would change. In other words, how important is it to use the most recent satellite information for input land use data series for integrated global modelling exercises. We took the old HYDE 3.1 reference maps of DISCover/GLC 2000 (Loveland and Belward, 1997; Loveland et al., 2000) valid for the reference year 2000, the IIASA/IFPRI cropland map (Fritz et al., 2015) valid for the reference year 2005 and the 2010 reference map (ESA, 2016) valid for the year 2010. Next, we ran a fuzzy numerical kappa analysis with the software from the Map Comparison Kit (Visser and de Nijs, 2006). The fuzzy numerical kappa analysis between the 2000 reference map (DISCover/GLC2000) and the 2010 reference map (ESA) yielded a substantial degree of agreement of 0.744 (1.00 = very high degree of agreement, 0.00 = very low). The comparison of the 2000 reference map (DISCover/GLC2000) with the 2005 reference map (IIASA/IFPRI) gave a fuzzy numerical kappa value of 0.727. Furthermore, the comparison between the 2005 reference map (IIASA/IFPRI) and the 2010 reference map (ESA) yielded a fuzzy numerical kappa value of 0.810. This means that there is overall a substantial agreement (or in other words relatively little difference) between the three reference maps for cropland. The fuzzy numerical kappa analysis between the 2000 reference map (DISCover/GLC2000) and the 2010 reference map (ESA) was 0.635. The comparison between the 2005 reference map (IIASA/IFPRI) and the 2010 reference map (ESA) yielded a kappa fuzzy numerical of 0.643. There is no grazing land map of 2005 from IIASA/IFPRI.

All this is in agreement with a study of 43 simulations from 11 global-scale land use–land change models of Prestele et al. (2016), showing that cropland is more consistent among the different reference starting conditions than grazing land. However, differences do exist, usually on the local scale. First, the original satellite input is different between the three data sets, with different sensors. Second, different algorithms were used to classify the land cover

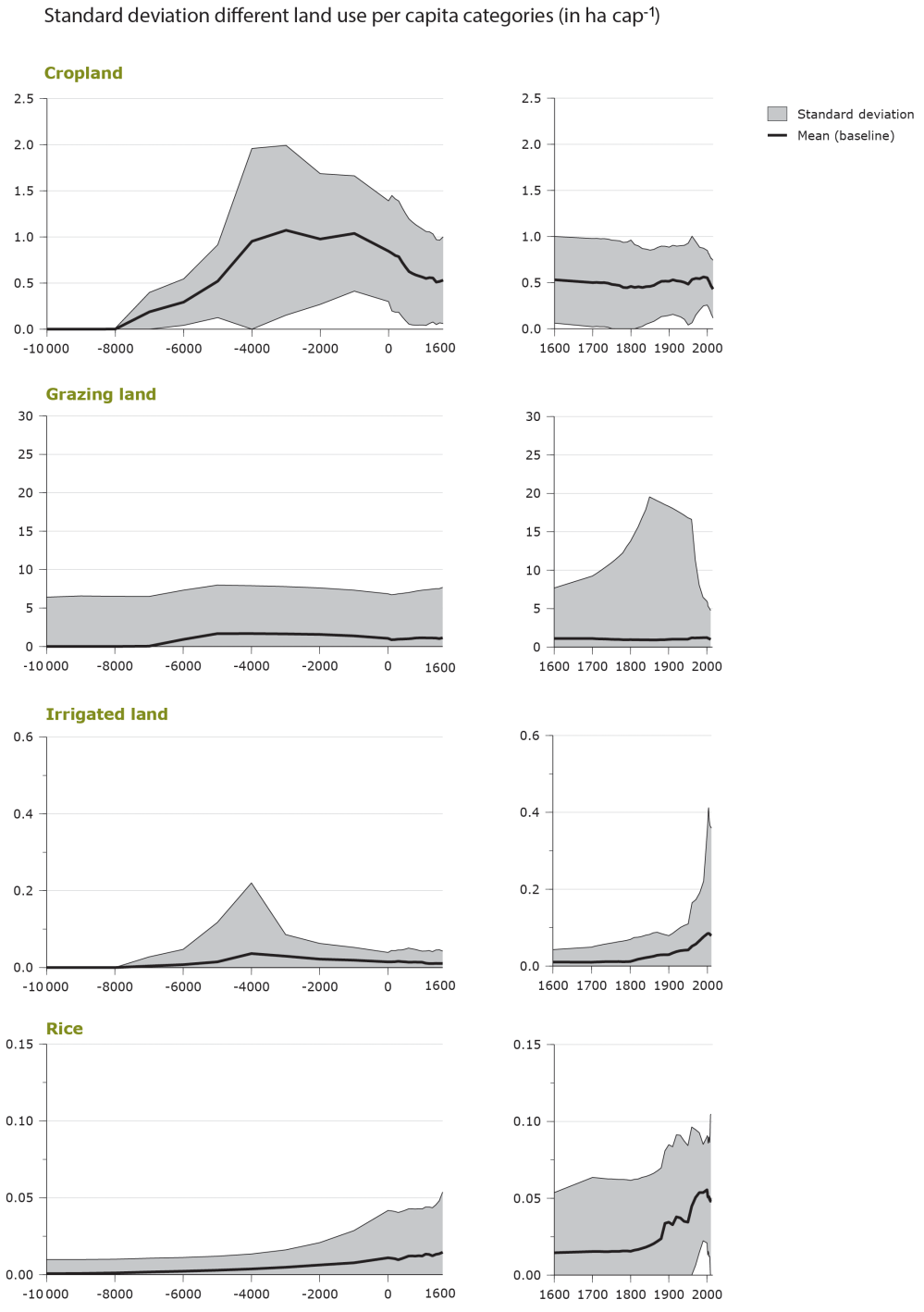

Figure 11. Standard deviation of input data per capita.

classes, which also led to different results. Third, when time progresses, the absolute areas of cropland have sometimes changed over time, either by expansion or abandonment, leading to different maps. We believe that for this hindcasting study, it does not play an important role which reference map we used, but it can be important for future modelling studies.

Finally, an important point to be made is that in this HYDE 3.2 version no empirical data are systematically used (yet) to improve the historical land use reconstructions. All allocation in the distant past is performed following general, globally applicable HYDE allocation rules. As Morrison (2015) rightly pointed out, these rules are often made with a Eurocentric point of view. We fully acknowledge this

Table 6. Summary of global population and land use estimates.

Historical global population (million) land use estimates (million ha).								
	5000 BCE	1 CE	500 CE	1000 CE	1500 CE	1700 CE	1850 CE	2015 CE
Population	19.0	232	253	323	503	592	1271	7301
Cropland	5.8	145	133	162	256	293	578	1591
Rain-fed area	5.6	142	129	157	252	289	549	1316
Net irrigated area	0.2	3	3	4	4	4	28	276
Net rice area	0.1	3	3	5	9	12	28	118
Paddy rice	0.0	1	1	2	2	3	12	75
Rain-fed rice	0.1	2	2	3	6	10	16	43
Grazing	30.1	199	249	366	515	664	1192	3241
Pasture	0.0	17	15	55	105	145	253	787
Rangeland	30.0	181	234	310	410	519	939	2454
% agric/total land area	0.3 %	2.6 %	2.9 %	4.0 %	5.9 %	7.3 %	13.6 %	37.1 %

since these rules were used as a first simple attempt to allocate land use in the distant past. We are aware that there is a need for a much more regionalized approach. Very promising work is underway in the Past Global Change (PAGES, http://www.pages.org/) LandCover6K working group initiative, for which archaeologists, historians, geographers, paleoecologists and land use reconstructors join efforts for the first time to collect and provide rich data from all different disciplines in order to improve the ALCC time series. In return, this is beneficial for several model intercomparison projects such as the Coupled Model Intercomparisons Project (CMIP) and the Land Use Model Intercomparison Project (LUMIP), which aim to further advance understanding of the impacts of land use and land cover change on climate (Lawrence et al., 2016).

6 Data availability

This HYDE version replaces earlier beta releases as provided at DANS DOI https://doi.org/10.17026/dans-25g-gez3. All data can be downloaded from ftp://ftp.pbl.nl/hyde/hyde3.2/ and supplementary data can be downloaded from ftp://ftp.pbl.nl/hyde/supplementary/Klein_Goldewijk_et_al_2017_HYDE32_paper/.

7 Discussion

We have estimated population and specific land use categories for the Holocene. Population has grown exponentially; however, while growth rates were initially very low, only during the last century did they dramatically increase to more than 1 %. Grazing land and cropland also increased but at a slower rate. The majority of cropland is rain-fed, but irrigated croplands and rice areas – despite their relatively small share – have been a very important factor in the increase in yield and production. We have estimated that total agricultural land occupied less than 0.5 % of the total land area in 5000 BCE, 3.4 % in 1 CE, 13.6 % in 1850 CE and 37.4 % in 2015 CE. Table 6 summarizes our estimates for population and land use for the Holocene.

This and the few other existing global estimates of historical land use are rather uncertain (Klein Goldewijk and Verburg, 2013). This can partly be explained by the sheer lack of reliable data, and hence by the large difference in methods and assumptions used for reconstruction. Most estimates of historic land use cover the period from today back to 1700; only two go further back in time (Pongratz et al., 2008, Kaplan et al., 2010). In general, the core of the methodology is regional and national or subnational estimates of historic cropland and pasture areas, which are allocated on a grid in a hindcasting mode starting from today's land cover. Similar to the HYDE methodology, the estimates of cropland and pasture areas are a mix of original data on agricultural area and calculations based on population data and assumed cropland per capita factors in time.

For example, Ramankutty and Foley (1999) present a simple approach to derive geographically explicit changes in global croplands from 1700 to 1992 CE. They created a global representation of permanent croplands in 1992 CE at 5′ spatial resolution by calibrating a remotely sensed land cover classification data set against cropland inventory data. Then, from a variety of sources, they compiled an extensive database of historical cropland inventory data, at the national and subnational level. Next, they hindcasted the 1992 CE data with a simple land use change model back to 1700 CE. Recently, the data set was updated to 2007 and revised. The range in cropland estimates (see Table 2) mostly originates from different definitions of cropland area. Pongratz et al. (2008), who covered the time period 800–1992 CE, already show higher cropland areas in the 20th century, and this is maintained for the entire historic period.

Table 7. Comparison total agricultural land estimates: HYDE 3.2 and Kaplan et al. (2011).

Total agricultural land (Mha)									
	4000 BCE	1000 BCE	1 CE	100 CE	500 CE	1000 CE	1500 CE	1600 CE	1850 CE
HYDE 3.2	62	200	344	355	382	527	771	850	1769
Kaplan et al. (2010)	186	871	1360	1440	1530	1800	2300	2160	2940

On a grid cell level, further difference between historic land use products can arise. Most methods use simple land use change models with specific, partly socio-economic suitability factors. Additionally, various assumptions are made as to which natural vegetation type is preferentially converted to agriculture (see also Prestele et al., 2016), i.e. whether agricultural land is taken preferentially from the forested, grass-covered or shrub-covered parts of the grid cell; this decision can cause large differences in the reconstructed extent of natural vegetation types (Reick et al., 2013). For the Pongratz et al. (2008) reconstruction, allocation rules for cropland were derived from the existing high-resolution (5 arcmin) maps of cropland and potential vegetation, while pasture is first allocated to grass as far as possible, then to the area of the woody vegetation types. This procedure reflects the human behaviour of minimizing effort: clearing of forest is generally not performed if sufficient natural grassland is available for grazing (Houghton, 1999).

The hindcasting prior to 1700 CE is even more uncertain than the period thereafter, as data become increasingly scarce. Therefore, the only practical approach is to use population data and assumptions about per capita needs for agricultural land. A key factor in explaining differences between these estimates is temporal and spatial changes in per capita land requirements: earlier versions of the HYDE database kept per capita land use constant over time or, in the uncertainty estimates, homogeneously varied it with time across the globe; the KK10 (Kaplan et al., 2010) data set assumed that land use intensification depends on the development stage of a society, which was represented by population density (this relationship was derived from data for five European countries and applied to the globe). By contrast, Pongratz et al. (2008) used a wealth of literature on agricultural practices and agro-technological innovations for all regions in the world (note that such literature exists more readily for the last millennium as compared to the longer time periods HYDE and KK10 covered); with this, per capita land use estimates could be accounted for as evolving over time and at the same time changing differently in the different regions of the globe. This approach accounts for, for example, the spread of wet rice farming in China that drastically lowered per capita land needs over time, or the importance of hunting, gathering, and fishing in some of the traditional societies in the Americas.

In addition to the per capita need for agricultural land, population data are the second determining factor in our analysis. To account for their uncertainties, different population databases were used and the upper and lower ends of an uncertainty range were assessed. Together with the uncertainty range in per capita cropland, this led to two different trajectories of land cover change that reflect the upper and lower bounds within the uncertainty range of historical land cover changes, around the default estimate that used a specific population data set and assumed constant per capita land use changes over time.

A key shortcoming for application of the reconstruction on a fine spatial scale is the implicit assumption of constant land use patterns over time. While relative changes between countries are captured by the regionally specific population and per capita land use data, within a given country the pattern of agricultural extent from present day is kept fixed and simply scaled with national totals. Some regional adjustments have been made where this assumption has been known to not apply, e.g. the differential agricultural expansion of different parts of Russia or the arrival of Europeans to only specific parts of Australasian and North and South American countries.

The total amount of agricultural area computed by our study is significantly smaller than the estimate of Kaplan et al. (2011). This can largely be explained by differences in methodology; Kaplan et al. (2011) used a correlation between deforestation and population density, varying over time with changes in technology and development. It was calibrated for Europe and then extrapolated to the rest of the world, which very likely caused an overestimation of land use change estimates. Since HYDE 3.2 does not estimate anthropogenic activities such as wood harvesting or shifting cultivation, our resulting estimates of deforestation are also necessarily lower; see Table 7 for an overview of the total agricultural areas from both studies.

Despite all these uncertainties, there is a great need for historic land use reconstruction, especially in the climate change modelling community. Earlier versions of the HYDE database have been used in the Land-Use Harmonization (LUH) data sets (Hurtt et al., 2011), and this most recent HYDE 3.2 version is again applied in the follow-up product LUH2, complemented with future scenarios of land use change. These LUH data sets are specifically developed to meet the needs of integrated assessment models (IAMs) and Earth system models (ESMs) developing future scenarios and simulations as part of international assessment (IPCC's 5th Assessment Report and soon CMIP6 and the 6th Assess-

ment Report). IAMs produce estimates of future regional or gridded land use as part of their future scenario projections, while ESMs require spatio-temporal information on land use activities from at least 800 CE onwards, including estimates of secondary (recovering) land age, area and biomass density to quantify the impacts of human land use on the Earth system. The LUH data sets make sure that IAM future projections do smoothly transition from the end of historical reconstructions. In addition to the LUH data sets that are provided to the scientific community, in which model inputs and decisions are systematically varied and the resulting changes in model outputs are examined, large-scale sensitivity analyses are also performed. The analysis shows that our model is most sensitive to the historical start date, the choice of primary vs. secondary priority for land use conversions, and the inclusion of wood harvesting and shifting cultivation.

The LUH data, of which the HYDE database is an essential part, have now been used by almost all ESMs producing simulations for the CMIP5 experiments and the IPCC AR5 process (Brovkin et al., 2013; Jones et al., 2011; Shevliakova et al., 2009). The LUH data have also been used and highlighted in several other studies, e.g. Thomson et al. (2010), Pereira et al. (2010) and Jones et al. (2013). These studies have made use of the detailed land use transition information in the LUH products to quantify land conversion events and track the resulting demographic effects of land disturbance and recovery, ultimately helping to close regional and global carbon budgets as well as impacts on future biodiversity.

The Supplement related to this article is available online at https://doi.org/10.5194/essd-9-927-2017-supplement.

Competing interests. The authors declare that they have no conflict of interest.

Acknowledgements. We thank the reviewers for their constructive comments. This research was performed with the support of NWO grant no. 016.158.021. This study was also undertaken as part of the Past Global Changes (PAGES) LandCover6K working group project, which in turn received support from the US National Science Foundation and the Swiss Academy of Sciences.

Edited by: David Carlson
Reviewed by: two anonymous referees

References

Ara, I., Lewis, M., and Ostendorf, B.: Spatio-temporal analysis of the impact of climate, cropping intensity and means of irrigation: an assessment on rice yield determinants in Bangladesh, Agriculture & Food Security, 5, 12, https://doi.org/10.1186/s40066-016-0061-9, 2016.

Armesto, J. J., Manuschevich, D., Mora, A., Smith-Ramirez, C., Rozzi, R., Abarzua, A. M., and Marquet, P. A.: From the Holocene to the Anthropocene: A historical framework for land cover change in southwestern South America in the past 15,000 years, Land Use Policy, 27, 148–160, 2009.

Australian Bureau of Statistics: 7124.0 – Historical Selected Agriculture Commodities, by State (1861 to Present), Australian Goverment, Canberra office, Canberra, Australia, 2001.

Barker, G.: The archaeology of foraging and farming at Niah Cave, Sarawak, Asian Perspect., 44, 90–106, 2006.

Barker, R., Herdt, R. W., and Rose, B.: The Rice enconomy of Asia, Resources for the Future, John Hopkins Press, Washington D.C., 1985.

Bellwood, P.: Early Agriculturalist Population Diasporas? Farming, Languages, and Genes, Annu. Rev. Anthropol., 30, 181–207, 2001.

Bertrand, C. and Van Ypersele, J. P.: Transient climate simulation forced by natural and anthropogenic climate forcings, Int. J. Climatol., 22, 623–648, 2002.

Betts, R. A.: Forcings and feedbacks by land ecosystem changes on climate change, J. Phys. IV, 139, 119–142, https://doi.org/10.1051/jp4:2006139009, 2006.

Betts, R. A., Falloon, P. D., Klein Goldewijk, K., and Ramankutty, N.: Biogeophysical effects of land use on climate: Model simulations of radiative forcing and large-scale temperature change, Agr. Forest Meteorol., 142, 216–233, 2007.

Biraben: Essai sur l'évolution du nombre des hommes, Population, French Edn., 34, 13–25, 1979.

Biraben, J.-N.: An Essay Concerning Mankind's Evolution, Population, Springer USA, 1980.

Bogue, D. J.: The Population of the United States, Historical Trends and Future Projections, The Free Press, New York, 1985.

Braudel, F.: The structure of everyday life: The limits of the possible, University of California Press, Berkely CA, 1981.

Brovkin, V., Claussen, M., Driesschaert, E., Fichefet, T., Kicklighter, D., Loutre, M. F., Matthews, H. D., Ramankutty, N., Schaeffer, M., and Sokolov, A.: Biogeophysical effects of historical land cover changes simulated by six Earth system models of intermediate complexity, Clim. Dynam., 26, 587–600, 2006.

Brovkin, V. L., Boysen, L., Arora, V. K., Boisier, J. P., Cadule, P., Chini, L., Claussen, M., Friedlingstein, P., Gayler, V., van den Hurk, B., Hurtt, G., Jones, C., Kato, E., de Noblet-Ducoudré, N., Pacifico, F., Pongratz, J., and Weiss, M.: Effect of anthropogenic land-use and land cover changes on climate and land carbon storage in CMIP5 projections for the 21st century, J. Climate, 26, 6859–6881, 2013.

Butzer, K. W.: Environment and archeology, an introduction to Pleistocene geography, Aldine Publishing Co., Chicago, 1964.

Caldwell, J. C. and Schindlmayr, T.: Historical population estimates: unraveling the Consensus, Popul. Dev. Rev., 28, 183–204, 2002.

China National Bureau of Statistics: http://www.stats.gov.cn/english, last access: 31 May 2008.

Clark, W. C.: Population geography, Prog. Hum. Geog., 1, 136–141, 1977.

Claussen, M., Brovkin, V., and Ganopolski, A.: Biophysical versus biogeochemical feedbacks of large-scale land cover change, Geophys. Res. Lett., 28, 1011–1014, 2001.

Coale, A. J.: Growth and Structure of Human Populations: A Mathematical Investigation, Princeton University Press, Princeton Legacy Library, New Jersey, USA, 1974.

Deevey, E. S.: The human population, Scientific American, CCIII, 195–204, 1960.

Denevan, W. M.: The native population of the Americas in 1492, University of Winsconsin Press, Madison, USA, 1992.

Durand, J. D.: Historical Estimates of World Population: An Evaluation, Popul. Dev. Rev., 3, 253–296, 1977.

Durand, J. D.: Historical Estimates of World Population: An Evaluation, PSC Analytical and Technical Reports Number 10, Table 2, University of Pennsylvania, Population Studies Center, Philadelphia, USA, 1974.

Ellis, E. C.: Ecology in an anthropogenic biosphere, Ecol. Monogr., 85, 287–331, 2015.

Ellis, E. C., Kaplan, J. O., Fuller, D. Q., Vavrus, S., Klein Goldewijk, K., and Verburg, P. H.: Used Planet: A Global History, P. Natl. Acad. Sci. USA, 110, 7978–7985, 2013.

Esser, G.: Osnabrück Biosphere Model: Structure, Construction, Results, in: Modern Ecology, Basic and Applied Aspects, edited by: Esser, G. and Overdieck, D., Elsevier Sci Publ., New York, 1991.

ESA: Three global LC maps for the 2000, 2005 and 2010 epochs, European Space Agency, available at: http://maps.elie.ucl.ac.be/CCI/viewer/index.php (last access: May 2017), 2016.

ETOPO5: 5-Minute Gridded Global Relief Data Collection (ETOPO5), NOAA-NGDC (Ed.), Boulder, Colorado, USA, 2005.

FAO: FAOSTAT, Food and Agriculture Organization of the United Nations, Rome, Italy, available at: http://www.fao.org, last access: June 2015.

Feddema, J. J., Oleson, K. W., Bonan, G. B., Mearns, L. O., Buja, L. E., Meehl, G. A., and Washington, W. M.: Atmospheric science: The importance of land-cover change in simulating future climates, Science, 310, 1674–1678, 2005.

Flint, E. P. and Richards, J. F.: Historical analysis of changes in land use and carbon stock of vegetation in South and Southeast Asia, Can. J. Forest Res., 21, 91–110, 1991.

Foley, J. A., DeFries, R., Asner, G. P., Barford, C., Bonan, G., Carpenter, S. R., Chapin, F. S., Coe, M. T., Daily, G. C., Gibbs, H. K., Helkowski, J. H., Holloway, T., Howard, E. A., Kucharik, C. J., Monfreda, C., Patz, J. A., Prentice, I. C., Ramankutty, N., and Snyder, P. K.: Global consequences of land use, Science, 309, 570–574, 2005.

Framji, K., Garg, B., and Lutrha, S.: Irrigation and drainage in the world – a global review, International Commission on Irrigation and Drainage, New Dehli, India, 1982.

Freydank, K. and Siebert, S.: Towards mapping the extent of irrigation in the last century: a time series of irrigated area per country, Universität Frankfurt am Main, Frankfurt, Germany, 2008.

Fritz, S., See, L., McCallum, I., You, L., Bun, A., Moltchanova, E., Duerauer, M., Albrecht, F., Schill, C., Perger, C., Havlik, P., Mosnier, A., Thornton, P., Wood-Sichra, U., Herrero, M., Becker-Reshef, I., Justice, C., Hansen, M., Gong, P., Abdel Aziz, S., Cipriani, A., Cumani, R., Cecchi, G., Conchedda, G., Ferreira, S., Gomez, A., Haffani, M., Kayitakire, F., Malanding, J., Mueller, R., Newby, T., Nonguierma, A., Olusegun, A., Ortner, S., Rajak, D. R., Rocha, J., Schepaschenko, D., Schepaschenko, M., Terekhov, A., Tiangwa, A., Vancutsem, C., Vintrou, E., Wenbin, W., van der Velde, M., Dunwoody, A., Kraxner, F., and Obersteiner, M.: Mapping global cropland and field size, Glob. Change Biol., 21, 1980–1992, 2015.

Frolking, S., Qiu, J., Boles, S., Xiao, X., Liu, J., Zhuang, Y., Li, C., and Qin, X.: Combining remote sensing and ground census data to develop new maps of the distribution of rice agriculture in China, Global Biogeochem. Cy., 16, 38–31, 2002.

Fuller, D. and Qin, L.: Pathways to Asian civilizations: Tracing the origins and spread of rice and rice cultures, Rice, 4, 78–92, 2011.

Fuller, D., Qin, Q., and Harvey, E.: A Critical Assessment of Early Agriculture in East Asia, with emphasis on Lower Yangtze Rice Domestication, Pradghara (Journal of the Uttar Pradesh State Archaeology Department), 18, 18–20, 2007.

Fuller, D., van Etten, J., Manning, K., Castillo, C., Kingwell-Banham, E., Weisskopf, A., Qin, L., Sato, Y.-I., and Hijmans, R. J.: The contribution of rice agriculture and livestock pastoralism to prehistoric methane levels: An archaeological assessment, The Holocene, 21, 743–759, 2011.

GAEZ: Joined Global Agro-Ecological Zones Project (GAEZ), FAO-IIASA, Laxenburg, Austria, available at: http://www.fao.org/ag/agl/agll/gaez/index.htm (last access: May 2015), 2000.

Gaillard, M.-J., Sugita, S., Mazier, F., Trondman, A.-K., Broström, A., Hickler, T., Kaplan, J. O., Kjellström, E., Kokfelt, U., Kuneš, P., Lemmen, C., Miller, P., Olofsson, J., Poska, A., Rundgren, M., Smith, B., Strandberg, G., Fyfe, R., Nielsen, A. B., Alenius, T., Balakauskas, L., Barnekow, L., Birks, H. J. B., Bjune, A., Björkman, L., Giesecke, T., Hjelle, K., Kalnina, L., Kangur, M., van der Knaap, W. O., Koff, T., Lagerås, P., Latalowa, M., Leydet, M., Lechterbeck, J., Lindbladh, M., Odgaard, B., Peglar, S., Segerström, U., von Stedingk, H., and Seppä, H.: Holocene land-cover reconstructions for studies on land cover-climate feedbacks, Clim. Past, 6, 483–499, https://doi.org/10.5194/cp-6-483-2010, 2010.

Ge, Q. S., Dai, J. H., He, F. N., Pan, Y., and Wang, M. M.: Land use changes and their relations with carbon cycles over the past 300 a in China, Sci. China Ser. D, 51, 871–884, 2008.

Grigg, D. B. (Ed.): The industrial revolution and land transformation, John Wiley, New York, 1987.

GYGA: Global Yield Gap and Water Productivity Atlas, Wageningen University, University of Nebraska, Water for Food, Daugherty Global Institute, Wageningen, 2017.

Hassan, F. A.: Demographic Archaeology: Studies in Archaeology, Academic Press, London, 1981.

Haub, C.: How many people have ever lived on Earth?, Population Today, 1995. 1995.

He, F., Li, S., and Zhang, X.: Reconstruction of cropland area and spatial distribution in the mid-Northern Song Dynasty (AD1004–1085), J. Geogr. Sci., 22, 359–370, 2012.

He, F., Li, S., Zhang, X., Ge, Q., and Dai, J.: Comparisons of cropland area from multiple datasets over the past 300 years in the traditional cultivated region of China, J. Geogr. Sci., 23, 978–990, 2013.

Hollman, R., Merchant, C. J., Saunders, R., Downy, C., Buchwitz, M., Cazenave, A., Chuvieco, E., Defourny, P., de Leeuw, G., Forsberg, R., Holzer-Popp, T., Paul, F., Sandven, S., Sathyendranath, S., van Roozendael, M., and Wagner, W.: The ESA climate change initiative, B. Am. Meteorol. Soc., 94, 1541–1552, https://doi.org/10.1175/BAMS-D-11-00254.1, 2013.

Houghton, R. A.: The annual net flux of carbon to the atmosphere from changes in land use 1850–1990, Tellus B, 51, 298–313, 1999.

Houghton, R. A. and Hackler, J. L.: Carbon Flux to the Atmosphere from Land-Use Changes: 1850 to 1990, Carbon Dioxide Information Analysis Center, U.S. Department of Energy, Oak Ridge National Laboratory, Oak Ridge, Tennessee, USA, 86 pp., 2002.

Houghton, R. A., Hobbie, J. E., Melillo, J. M., Moore, B., Peterson, B. J., Shaver, G. R., and Woodwell, G. M.: Changes in the Carbon Content of Terrestrial Biota and Soils between 1860 and 1980: A Net Release of CO_2 to the Atmosphere, Ecol. Monogr., 53, 236–262, 1983.

Hurtt, G. C., Chini, L. P., Frolking, S., Betts, R., Feddema, J. J., Fischer, G., Hibbard, K. A., Janetos, A. C., Jones, C., Klein Goldewijk, K., Kindermann, G., Kinoshita, T., Riahi, K., Shevliakova, E., Smith, S., Stehfest, E., Thomson, A., Thornton, P., van Vuuren, D., and Wang, Y. P.: Harmonization of land-use scenarios for the period 1500–2100: 600 years of global gridded annual land-use transitions, wood harvest, and resulting secondary lands, Climatic Change, 109, 117–161, 2011.

Indiastat: Statistics India, Ministry of Agriculture, Government of India, Datanet India Pvt. Ltd. D-100, First Floor, Okhla Industrial Area, Phase-I, New Delhi, 2009.

Jones, C. D., Hughes, J. K., Bellouin, N., Hardiman, S. C., Jones, G. S., Knight, J., Liddicoat, S., O'Connor, F. M., Andres, R. J., Bell, C., Boo, K.-O., Bozzo, A., Butchart, N., Cadule, P., Corbin, K. D., Doutriaux-Boucher, M., Friedlingstein, P., Gornall, J., Gray, L., Halloran, P. R., Hurtt, G., Ingram, W. J., Lamarque, J.-F., Law, R. M., Meinshausen, M., Osprey, S., Palin, E. J., Parsons Chini, L., Raddatz, T., Sanderson, M. G., Sellar, A. A., Schurer, A., Valdes, P., Wood, N., Woodward, S., Yoshioka, M., and Zerroukat, M.: The HadGEM2-ES implementation of CMIP5 centennial simulations, Geosci. Model Dev., 4, 543–570, https://doi.org/10.5194/gmd-4-543-2011, 2011.

Jones, A. D., W. Collins, W., Edmonds, J., Torn, M., Janetos, A., Calvin, K., Thomson, A., Chini, L., Mao, J., Shi, X., Thornton, P., Hurtt, G., and Wise, M.: Greenhouse gas policy influences climate via direct effects of land-use change, J. Climate, 26, 3657–3670, https://doi.org/10.1175/JCLI-D-12-00377.1, 2013.

Kalaiselvi, S. and Sundar, I.: Interstate Disparity in Cropping Intensity in India, International Journal of Business Management, Economics and Information Technology, 3, 269–273, 2011.

Kapitsa, S.: A model of world population growth as an experiment in systematic research (Model' rosta naseleniya zemli kak opyt sistemnogo issledovaniya), Voprosy Statistiki, 8, 46–57, 1997.

Kaplan, J. O., Krumhardt, K. M., Ellis, E. C., Ruddiman, W. F., Lemmen, C., and Klein Goldewijk, K.: Holocene carbon emissions as a result of anthropogenic land cover change, The Holocene, 21, 775–791, 2011.

Kaplan, J. O., Krunhardt, K. M., and Zimmermann, N.: The prehistoric and preindustrial deforestation of Europe, Quaternary Sci. Rev., 28, 3016–3034, 2009.

Klein Goldewijk, K.: Estimating global land use change over the past 300 years: The HYDE database, Global Biogeochem. Cy., 15, 417–433, 2001.

Klein Goldewijk, K. and Battjes, J. J.: The IMAGE Hundred Year (1890–1990) Database for Integrated Environmental Assessments (HYDE Version 1.0), National Institute of Public Health and the Environment (RIVM), Bilthoven, Report 482523001, 170 pp., 1995.

Klein Goldewijk, K. and Verburg, P. H.: Uncertainties in global-scale reconstructions of historical land use: an illustration using the HYDE data set, Landscape Ecol., 28, 861–877, 2013.

Klein Goldewijk, K., Beusen, A., and Janssen, P.: Long term dynamic modeling of global population and built-up area in a spatially explicit way: HYDE 3.1, The Holocene, 20, 565–573, 2010.

Klein Goldewijk, K., Beusen, A., van Drecht, G., and de Vos, M.: The HYDE 3.1 spatially explicit database of human induced land use change over the past 12,000 years, Global Ecol. Biogeogr., 20, 73—86, 2011.

Klein Goldewijk, K., Dekker, S. C., and van Zanden, J. L.: Per-capita estimations of long-term historical land use and the consequences for global change research, Journal of Land Use Science, 12, 313–337, https://doi.org/10.1080/1747423X.2017.1354938, 2017.

Kropelin, S., Verschuren, D., Lezine, A. M., Eggermont, H., Cocquyt, C., Francus, P., Cazet, J. P., Fagot, M., Rumes, B., Russell, J. M., Darius, F., Conley, D. J., Schuster, M., Von Suchodoletz, H., and Engstrom, D. R.: Climate-driven ecosystem succession in the Sahara: The past 6000 years, Science, 320, 765–768, 2008.

LandScan: Landscan Global Population Database, The 2012 Revision, Oak Ridge National Laboratory, Oak Ridge, Tennessee, available at: http://www.ornl.gov/landscan (last access: January 2015), 2014.

Lawrence, D. M., Hurtt, G. C., Arneth, A., Brovkin, V., Calvin, K. V., Jones, A. D., Jones, C. D., Lawrence, P. J., de Noblet-Ducoudré, N., Pongratz, J., Seneviratne, S. I., and Shevliakova, E.: The Land Use Model Intercomparison Project (LUMIP) contribution to CMIP6: rationale and experimental design, Geosci. Model Dev., 9, 2973–2998, https://doi.org/10.5194/gmd-9-2973-2016, 2016.

Le Quéré, C., Moriarty, R., Andrew, R. M., Peters, G. P., Ciais, P., Friedlingstein, P., Jones, S. D., Sitch, S., Tans, P., Arneth, A., Boden, T. A., Bopp, L., Bozec, Y., Canadell, J. G., Chini, L. P., Chevallier, F., Cosca, C. E., Harris, I., Hoppema, M., Houghton, R. A., House, J. I., Jain, A. K., Johannessen, T., Kato, E., Keeling, R. F., Kitidis, V., Klein Goldewijk, K., Koven, C., Landa, C. S., Landschützer, P., Lenton, A., Lima, I. D., Marland, G., Mathis, J. T., Metzl, N., Nojiri, Y., Olsen, A., Ono, T., Peng, S., Peters, W., Pfeil, B., Poulter, B., Raupach, M. R., Regnier, P., Rödenbeck, C., Saito, S., Salisbury, J. E., Schuster, U., Schwinger, J., Séférian, R., Segschneider, J., Steinhoff, T., Stocker, B. D., Sutton, A. J., Takahashi, T., Tilbrook, B., van der Werf, G. R., Viovy, N., Wang, Y.-P., Wanninkhof, R., Wiltshire, A., and Zeng, N.: Global carbon budget 2014, Earth Syst. Sci. Data, 7, 47–85, https://doi.org/10.5194/essd-7-47-2015, 2015.

Li, Y., Thenkabail, P. S., Biradar, C. M., Noojipady, P., Dheeravath, V., Velpuri, M., Gangalakunta, O., and Cai, X. L.: History of irrigated areas in the world, in: Global croplands for food security, edited by: Thenkabail, P. S., Lyon, J. G., Turral, H., and Biradar, C. M., CRC Press, Taylor and Francis Group, Boca Raton, FL, USA, 2009.

Livi-Bacci, M.: A concise history of world population, 4th Edn., Blackwell Publishing, Oxford, UK, 2007.

Loveland, T. R. and Belward, A. S.: IGBP-DIS global 1 km land cover data set, DISCover: First results, Int. J. Remote Sens., 18, 3289–3295, 1997.

Loveland, T. R., Reed, B. C., Brown, J. F., Ohlen, D. O., Zhu, Z., Yang, L., and Merchant, J. W.: Development of a global land cover characteristics database and IGBP DISCover from 1 km AVHRR data, Int. J. Remote Sens., 21, 1303–1330, 2000.

Lucas, D.: Chapter three, World Population Growth, The Australian National University,Canberra, New South Wales, Australia, 2003.

Maddison, A.: The world economy: a millennial perspective, OECD, Paris, France, 2001.

McEvedy, C. and Jones, R.: World Atlas of population history, Penguin Books Ltd., Hammondsworth, UK, 1978.

Merrick, T. W.: World population in transition, Population Bulletin, 41, 53 pp., 1986.

Michael, A. M.: Irrigation: Theory and Practice, Vikas Publishing House PVT ltd, New Delhi, 2008.

Mitchell, B. R.: International Historical Statistics, Africa, Asia & Oceania: 1750–2005, 5th Edn., Palcrave MacMillan, New York, USA, 2007a.

Mitchell, B. R.: International Historical Statistics, Europe: 1750–2005, 6th Edn., Palcrave MacMillan, New York, USA, 2007b.

Mitchell, B. R.: International Historical Statistics, The Americas: 1750–2005, 6th Edn., Palcrave MacMillan, New York, USA, 2007c.

Morrison, K.: Provincializing the Anthropocene, Seminar, 673, 75–80, 2015.

Natural Earth: ne_10m_rivers_lake_centerlines, edited by: Natural Earth, http://www.naturalearthdata.com, last access: January 2015.

New, M., Hulme, M., and Jones, P.: A 1961–1990 mean monthly climatology of global land areas. Climate Research Unit, edited by: University of East Anglia, Norwich, 1997.

NLWRA: National Land and Water Resources Audit 2001, Australian Natural Resources Atlas, V 2.0., Land, Land Use Australia, 2001.

Olofsson, J. and Hickler, T.: Effects of human land-use on the global carbon cycle during the last 6,000 years, Veg. Hist. Archaeobot., 17, 605–615, 2008.

Olson, D. M., Dinerstein, E., Wikramanayake, E. D., Burgess, N. D., Powell, G. V. N., Underwood, E. C., D'Amico, J. A., Itoua, I., Strand, H. E., Morrison, J. C., Loucks, C. J., Allnutt, T. F., Ricketts, T. H., Kura, Y., Lamoreux, J. F., Wettengel, W. W., Hedao, P., and Kassem, K. R.: Terrestrial Ecoregions of the World: A New Map of Life on Earth, BioScience, 51, 933–938, 2001.

Opferkuch, K.: Quantifying Historical Rice Patterns. An evaluation and development of the current HYDE total rice agricultural area maps for the Southeast Asian region, Utrecht University, Utrecht, 2016.

Pacala, S. W., Hurtt, G. C., Baker, D., Peylin, P., Houghton, R. A., Birdsey, R. A., Heath, L., Sundquist, E. T., Stallard, R. F., Ciais, P., Moorcroft, P., Caspersen, J. P., Shevliakova, E., Moore, B., Kohlmaier, G., Holland, E., Gloor, H., Harmon, M. E., Fan, S. M., Sarmiento, J. L., Goodale, C. L., Schimel, D., and Field, C. B.: Consistent land- and atmosphere-based U.S. carbon sink estimates, Science, 292, 2316–2320, 2001.

Pereira, H. M., Leadley, P. W., Proença, V., Alkemade, R., Scharlemann, J. P. W., Fernandez-Manjarrés, J. F., Araújo, M. B., Balvanera, P., Biggs, R., Cheung, W. W. L., Chini, L., Cooper, H. D., Gilman, E. L., Guénette, S., Hurtt, G. C., Huntington, H. P., Mace, G. M., Oberdorff, T., Revenga, C., Rodrigues, P., Scholes, R. J., Sumaila, U. R., and Walpole, M.: Scenarios for Global Biodiversity in the 21st Century, Science, 2010. 1496–1501, 2010.

Pongratz, J., Reick, C., Raddatz, T., and Claussen, M.: A reconstruction of global agricultural areas and land cover for the last millennium, Global Biogeochem. Cy., 22, GB3018, https://doi.org/10.1029/2007GB003153, 2008.

Pongratz, J., Raddatz, T., Reick, C. H., Esch, M., and Claussen, M.: Radiative forcing from anthropogenic land cover change since A.D. 800, Geophys. Res. Lett., 36, L02709, https://doi.org/10.1029/2008GL036394, 2009.

Poulter, B., MacBean, N., Hartley, A., Khlystova, I., Arino, O., Betts, R., Bontemps, S., Boettcher, M., Brockmann, C., Defourny, P., Hagemann, S., Herold, M., Kirches, G., Lamarche, C., Lederer, D., Ottlé, C., Peters, M., and Peylin, P.: Plant functional type classification for earth system models: results from the European Space Agency's Land Cover Climate Change Initiative, Geosci. Model Dev., 8, 2315–2328, https://doi.org/10.5194/gmd-8-2315-2015, 2015.

Prentice, I. C., Cramer, W., Harrison, S. P., Leemans, R., Monserud, R. A., and Solomon, A. M.: A global biome model based on plant physiology and dominance, soil properties and climate, J. Biogeogr., 19, 117–134, 1992.

Prestele, R., Alexander, P., Rounsevell, M. D. A., Arneth, A., Calvin, K., Doelman, J., Eitelberg, D. A., Engström, K., Fujimori, S., Hasegawa, T., Havlik, P., Humpenöder, F., Jain, A. K., Krisztin, T., Kyle, P., Meiyappan, P., Popp, A., Sands, R. D., Schaldach, R., Schüngel, J., Stehfest, E., Tabeau, A., Van Meijl, H., Van Vliet, J., and Verburg, P. H.: Hotspots of uncertainty in land-use and land-cover change projections: a global-scale model comparison, Glob. Change Biol., 22, 3967–3983, https://doi.org/10.1111/gcb.13337, 2016.

Ramankutty, N.: Global Cropland and Pasture Data from 1700–2007, McGill University (Ed.), Montreal, Canada, 2012.

Ramankutty, N. and Foley, J. A.: Estimating historical changes in global land cover: Croplands from 1700 to 1992, Global Biogeochem. Cy., 13, 997–1027, 1999.

Reick, C. H., Raddatz, T., Brovkin, V., and Gayler, V.: Representation of natural and anthropogenic land cover change in MPI-ESM, Journal of Advances in Modelling Earth Systems, 5, 459–482, 2013.

Renfrew, C. and Bahn, P.: Archaeology: Theories, Methods & Practices, Thames & Hudson Ltd., 2008.

Richards, J. F.: Land transformation, Chapter 10, in: The Earth as transformed by human action, Turner, B. L., Clark, W. C., Kates, R. W., Richards, J. F., Mathews, J. T., Meyer, W. B., Cambridge University Press, New York, 1990.

Ricepedia: http://ricepedia.org/rice-around-the-world, last access: February 2015.

Siebert, S.: Technical Report documentation irrigation 17900–1900, University of Bonn, Bonn, 2008.

Siebert, S., Kummu, M., Porkka, M., Döll, P., Ramankutty, N., and Scanlon, B. R.: A global data set of the extent of irrigated land from 1900 to 2005, Hydrol. Earth Syst. Sci., 19, 1521–1545, https://doi.org/10.5194/hess-19-1521-2015, 2015.

Stern, D. I. and Kaufmann, R. K.: Estimates of global anthropogenic sulphate emissions 1860–1993, Center for Energy and Environmental Studies, Boston, Mass, 1996.

Sojka, R. E., Bjorneberg, D. L., and Entry, J. A.: Irrigation: an historical perspective, in: Encyclopedia of Soil Science, Marcel Dekker Inc., 2002. Tanton, J. H.: End of the migration epoch, The Social Contract, IV and V, 1995.

Tett, S., Betts, R., Crowley, T. J., Jones, A., Gregory, J., Oestroem, E., Roberts, D. L., and Woodage, M. J.: Simulating the recent holocene, American Meteorological Society, San Diego, CA, 2021–2029, 2005.

Thomlinson, R.: Demographic problems, controversy over population control, 2nd Edn., Dickenson Publishing Company, CA, 1975.

Tuve, G. L.: Energy, environment, population, and food, Wiley-Interscience, New York, 1976.

UN: Long-range world population projections: Two centuries of population growth, 1950–2150, United Nations Population Division, New York, 1992.

UN: World Population Prospects, The 2003 Revision, United Nations Population Division, New York, 2004.

UN: World Population Prospects, The 2007 Revision, United Nations Population Division, New York, 2008.

UNEP/WCMC: World Database on Protected Areas (WDPA). Protected Areas Programme, Cambridge, UK, 2013.

Urquhart, M. and Buckley, K.: Historical statistics of Canada, University Press, Toronto, Canada, 1965.

USDA: National Agricultural Statistics Service (NASS), http://www.nass.usda.gov (last access: June 2009), 2006.

Van Beek, L. H. P. and Bierkens, M. F. P.: The global hydrological model PCR-GLOBWB: conceptualization, parameterization and verification, Department of Physical Geography, Faculty of Earth Sciences, Utrecht University, Utrecht, 2008.

van Loon, H.: The story of mankind, New York, Liveright, 1922.

Vazquez-Presedo, V.: Estadisticas Historicas Argentinas (Comparadas), Buenos Aires Acad. Nacional de Ciencias Econoìmicas, Buenos Aires, Argentina, 1988.

Verburg, P. H., van de Steeg, J., Veldkamp, A., and Willemen, L.: From land cover change to land function dynamics: A major challenge to improve land characterization, J. Environ. Manage., 90, 1327–1335, 2009.

Verschuren, D., Lalrd, K. R., and Cumming, B. F.: Rainfall and drought in equatorial east Africa during the past 1,100 years, Nature, 403, 410–414, 2000.

Verschuren, D., Johnson, T. C., Kling, H. J., Edgington, D. N., Leavitt, P. R., Brown, E. T., Talbot, M. R., and Hecky, R. E.: History and timing of human impact on Lake Victoria, East Africa, P. Roy. Soc. B-Biol. Sci., 269, 289–294, 2002.

Visser, H. and de Nijs, T.: The Map Comparison Kit, Environ. Modell. Softw., 21, 346–358, 2006.

Waldner, F., Fritz, S., Di Gregorio, A., Plotnikov, D., Bartalev, S., Kussul, N., Gong, P., Thenkabil, P., Hazeu, G., Klein , I., Loew, F., Miettinen, J., Dadhwal, V. K., Lamarche, C., Bontemps, S., and Defourny, P.: A Unified Cropland Layer at 250 m for Global Agriculture Monitoring, Data, 1, 3, https://doi.org/10.3390/data1010003, 2016.

Wiens, T.: Agriculture and Rural Poverty in Vietnam, in: Household Wellfare and Vietnam's Transition, edited by: Dollar, D., Glewwe, P., and Litvack, J. I., World Bank, Washington, USA, 1998.

Williams, M.: Dark ages and dark areas: Global deforestation in the deep past, J. Hist. Geogr., 26, 28–46, 2000.

World Atlas of Agriculture: World Atlas of Agriculture, Istituto Geografico De Agostini S.p.A., Novara, Italy, 1969.

Woytinsky, W. S. and Woytinsky, E. S.: World Population and Production, The Lord Baltimore Press, New York, 1953.

You, L., Wood-Sichra, U., Fritz, S., Guo, Z., See, L., and Koo, J.: Spatial Production Allocation Model (SPAM) 2005 v2.0, available at: http://mapspam.info (last access: May 2015), 2014.

Zhang, J. and Wang, X.: Notes on the recent discovery of ancient cultivated rice at Jiahu, Henan Province: a new theory concerning the origin of Oryza japonica in China, Antiquity, 72, 897–901, 1998.